2002

A study of Amino acid 143 and 278 in the Vitamin D nuclear receptor

Karen Davis
San Jose State University

A Study of Amino Acids 143 and 278 in the Vitamin D Nuclear Receptor

A Thesis

Presented to

The Faculty of the Department of Chemical Engineering

San Jose State University

In Partial Fulfillment

of the Requirements for the Degree

Master of Science

By

Karen Davis

August 2002

Advisor Dr. Elaine D. Collins

UMI Number: 1410412

ProQuest Information and Learning Company
300 North Zeeb Road
P.O. Box 1346
Ann Arbor, MI 48106-1346

APPROVED FOR THE DEPARTMENT OF CHEMICAL ENGINEERING

Elaine D. Collins 6/20/02

Dr. Elaine D. Collins

Melanie A. McNeil 6/20/02

Dr. Melanie McNeil

Pamela C. Stacks 6/20/2002

Dr. Pam Stacks

APPROVED FOR THE UNIVERSITY

[signature]

ABSTRACT

A Study of Amino Acids 143 and 278 in the Vitamin D Nuclear Receptor

by Karen Davis

Vitamin D is actually a steroid hormone, and its most biologically active form is 1,25-dihydroxyvitamin D_3 [$1,25(OH)_2D_3$]. Its action in the human body is mediated by binding to the vitamin D nuclear receptor (VDR), a protein. This research investigates the binding affinity of $1,25(OH)_2D_3$ to receptors with mutated amino acids. Site-directed mutagenesis was used to generate two single point mutants, Y143F, and S278A, and a double mutant, Y143F/S278A. The variant VDR proteins were analyzed by performing binding assays, and calculating K_d. K_d values were determined to be 0.788 +/- 0.058 nM for wild type VDR, 0.896 +/- 0.168 nM for Y143F VDR, 1.24 +/- 0.316 nM for S278A VDR and 1.28 +/- 0.383 nM for Y143F/S78A VDR. This data indicates that there is not a significant difference in the binding affinity of $1,25(OH)_2D_3$ when the 143 or 278 residues are mutated, implying that neither residue is critical for binding $1,25(OH)_2D_3$.

Acknowledgements

I would like to thank Dr. Elaine Collins for her invaluable assistance in performing this research. She has been extremely generous with her time and knowledge during the eighteen months of this project, and willing to demonstrate the many techniques that I needed to learn in order to perform this research.

I would also like to thank my children Jessica and Alex for their patience and tolerance throughout five semesters of night classes and schoolwork that consumed my time at home. Their support has allowed me to complete my degree and pursue new career options.

Table of Contents

Chapter	Page
1.0 Introduction	1
2.0 Literature Review	9
2.1 Categorization of Literature	9
2.2 Analog Studies	12
2.3 Site-Directed Mutagenesis Studies	15
2.4 Crystallography Data of VDR	22
2.5 Models of VDR	24
2.6 Summary of Literature Review	29
3.0 Research Hypothesis and Objective	31
3.1 Research Hypothesis	31
3.2 Research Objective	31
4.0 Methods and Materials	33
4.1 Buffers and Solutions	33
4.2 Site-directed Mutagenesis	33
4.3 Bacterial Cell Transformation	35
4.4 Plasmid Mini-preparations	35
4.5 Restriction Digest	36
4.6 DNA Sequencing	37
4.7 Large Plasmid Prep	38
4.8 Cell Culture	39

4.9 Transfection of COS-1 Cells 39

4.10 Harvesting of COS-1 Cells 40

4.11 Binding Assays 40

5.0 Results 43

5.1 Site-directed Mutagenesis and Sequencing 43

5.2 Binding Assays 44

5.3 Statistical Analysis of Data 52

6.0 Discussion 54

7.0 Conclusion 61

8.0 References 62

Appendices:

A. VDR Amino Acid Sequence and One Letter Amino Acid Abbreviations 75

A1. Vitamin D Nuclear Receptor Amino Acid Sequence 75

A2. Single Letter Abbreviations for Amino Acids 75

B. pcDNA 1.1/Amp Plasmid Map 76

C. Sequencing Data of Entire VDR Gene for Mutants 77

D. Raw Data of Binding Assays-DPM 80

List of Tables

Table **Page**

Table 1- Amino Acid Residues Involved in Hydrogen Binding to OH Group of $1,25(OH)_2D_3$ 7

Table 2- VDRE Nucleotide Sequences in VDR-Regulated Genes..... 12

Table 3- K_d Data for $1,25(OH)_2D_3$ Binding with F244G, K246G,K246G, L254G, Q259G, L262G Mutated VDR..... 17

Table 4- K_d Data for $1,25(OH)_2D_3$ Binding with C288G, C337G, and C369G Mutated VDR..... 19

Table 5- Summary of Mutational Analysis of LBD of VDR..... 20

Table 6- Comparison of VDR X-ray Crystallography Data and VDR Models..... 28

Table 7- Primers Used for Site-Directed Mutagenesis and Sequencing 34

Table 8- Beckman LS6500 Scintillation Counter Settings for Binding Assay Measurements..... 42

Table 9- Summary Data of Binding Assays 52

Table 10- Statistical Summary of Binding Assay Trials..... 53

List of Figures

Figure **Page**

Figure 1- Vitamin D_2 and Vitamin D_3 structure 2

Figure 2- 1,25$(OH)_2$-Vitamin D_3 4

Figure 3- The Domain Structure of VDR. 6

Figure 4- Ring Conformations of 1,25$(OH)_2D_3$ 8

Figure 5- Percent Maximal Binding of 1,25$(OH)_2D_3$ for Mutations in VDR 16

Figure 6- Comparing Models of the Ligand Binding Domain 25

Figure 7- Sequencing Gel Showing GCC Mutation of VDR S278A DNA 44

Figure 8- Saturation Analysis of Wild Type Mutant 47

Figure 9- Saturation Analysis of 143 Mutant 48

Figure 10- Saturation Analysis of 278 Mutant 49

Figure 11- Saturation Analysis of 143/278 Mutant 50

Figure 12- Specific Binding Curves for 143, 278, 143/278 and Wild Type VDR..... 51

1.0 Introduction

Vitamin D has many roles in the human body, but was first discovered in connection to the disease rickets. The advent of the Industrial Revolution in Britain in the late 1700's brought about a significant increase in the occurrence of this disease (Collins & Norman, 2001). Rickets is characterized by bowed legs, knock-knees, and delayed walking in children. The bones of rickets patients are "too soft" due to insufficient calcium needed for mineralization of the bone matrix. Rachitic children also suffer from painful spasms of the hands, feet, and larnyx, known as tetany (Blilezikian, Raisz, & Rodan, 1996). In the late 1800's, several researchers published studies connecting rickets to low sunlight exposure and noted that large cities in northern latitudes had the highest rates of the disease (Palm, 1890; Owen, 1899).

In 1918, Sir Edward Mellanby conducted experiments with dogs and concluded that the recently discovered Vitamin A in cod-liver oil was the source of the rickets cure (Collins & Norman, 2001). However, experiments done in 1922 demonstrated that Vitamin A was not the antirachitic substance, and the newly identified cure was called "Vitamin D" (McCollum, Simmonds, Becker, & Shipley, 1922). In the same timeframe, German researcher K. Huldschinsky was able to cure children of rickets using artificially produced ultraviolet light treatment (Conlan & Sherman, 2001). By 1924, foods like milk and bread were being irradiated with ultraviolet light, and the incidences of the disease were greatly reduced (Steenbock, 1924).

The connection to ultraviolet light exposure eventually led to the discovery that Vitamin D was not a true vitamin. A vitamin is defined as an essential nutrient that the

body cannot manufacture, but vitamin D can be produced in the body. Two forms of vitamin D were discovered: D_2 (ergocalciferol), which could be produced by ultraviolet radiation of the plant sterol ergosterol, and D_3 (cholecalciferol), which could be produced in the body by irradiating 7-dehydrocholesterol (Askew, Bourdillon, Burce, Jenkins &, Webster, 1931; Windhaus, Schenck, & von Werder, 1936). 7-dehydrocholesterol is present in the body as a biosynthesis product of cholesterol, and it was discovered that vitamin D is produced in the body by the action of UV light on 7-dehydrocholesterol. Ergocalciferol is the form of vitamin D found in irradiated foods, while cholecalciferol is the form found in cod-liver oil (Askew *et al.*, 1931). The chemical structures of vitamins D_2 and D_3 are shown in Figure 1.

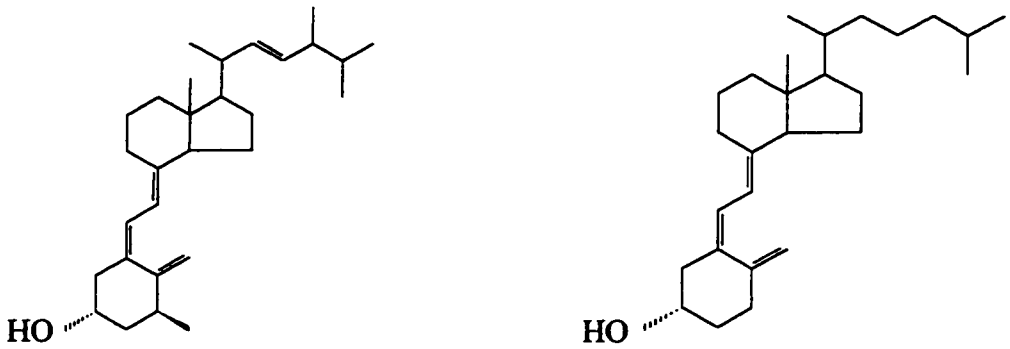

Vitamin D_2 (ergocalciferol) Vitamin D_3 (cholecalciferol)

Figure 1- Vitamin D_2 and Vitamin D_3 Structure

The isolation and identification of the chemical structures of D_2 and D_3 did not solve the mystery of how vitamin D_3 was involved in the mineralization of bone. A general understanding of the physiologic function of vitamin D_3 (Nicolaysen & Eeg-Larsen,

1953) was developed with the conclusions that vitamin D_3 functioned directly without any further metabolism (Kodieck, 1956). This assumption was proven to be incorrect with the development of radiolabeled vitamin D_3 in high enough specific radioactivity to permit experiments with truly physiological amounts of vitamin D_3 (Deluca, 1995). The isolation and identification of 25-hydroxyvitamin D_3 as a modified form of vitamin D_3 produced in the liver followed (Blunt, DeLuca, & Schones, 1968). During the next few years, three separate research groups identified a second metabolite produced in the kidney (Fraser & Kodieck, 1970; Gray, Boyle, & DeLuca, 1971; Norman, Midgett, Myrtle, & Nowick, 1971). This biologically active form of vitamin D_3 was identified as 1,25-dihydroxyvitamin D_3 [$1,25(OH)_2D_3$]. (See Figure 2 for the structure of 1,25-dihdroxyvitamin D_3).

Hydroxylation takes place in two steps in the liver and the kidney. The liver hydroxylates vitamin D_3 to 25-hydroxyvitamin D_3, and then the kidney converts this compound to $1,25(OH)_2D_3$. The liver performs the conversion to 25-hydroxyvitamin D_3 on all vitamin D_3 available, while the kidney hydroxylation is much more tightly regulated. The $1,25(OH)_2D_3$ is released from the kidney and circulates in the blood bound to a carrier protein, vitamin D-binding protein (Henry *et al.*, 1992). As a result of these experiments, $1,25(OH)_2D_3$ was reclassified as a hormone that controlled calcium metabolism. A hormone is a chemical substance produced by one organ, and then transported in the bloodstream to a target organ, where it causes specific biological actions.

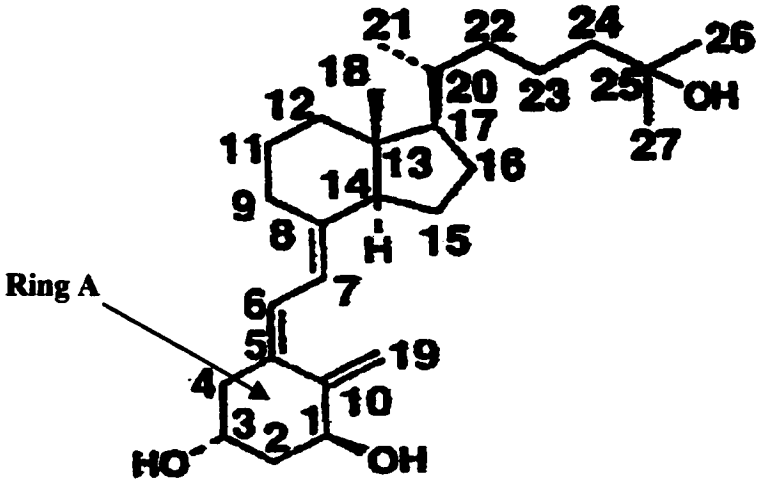

Figure 2- 1,25(OH)$_2$-Vitamin D$_3$. Structure with numbering scheme.

The most studied actions of 1,25(OH)$_2$D$_3$ involve the regulation of calcium and phosphate in the body. 1,25(OH)$_2$D$_3$ stimulates intestinal calcium and phosphate absorption, and bone calcium and phosphate resorption. Serum calcium and phosphate ion concentrations are crucial for mineralization of the organic bone matrix.

In 1975, Mark Haussler made the discovery that a protein receptor in the nucleus of cells in the intestine binds the 1,25(OH)$_2$D$_3$ ligand (Haussler & Brumbaugh, 1975). This vitamin D receptor (VDR) is a ligand-dependent transcription factor that alters target gene expression. The bound ligand produces conformational changes in the VDR (Peleg, Sastry, Collins, Bishop, & Norman, 1995), which enable the VDR to interact with coactivator multiprotein complexes. The result of these interactions is to facilitate the binding of RNA polymerase II complex to DNA, inducing gene transcription in many target genes. Binding can also inhibit the expression of genes. Nuclear receptors for

$1,25(OH)_2D_3$ have since been found to be present in many other tissues. Some of the additional tissues identified are brain, pancreas, pituitary, skin, muscle, parathyroid, prostate, and immune cells.

In the 1980's, $1,25(OH)_2D_3$ was shown to inhibit skin cells growth, and topical applications of $1,25(OH)_2D_3$ or an analog were proved to be effective as a treatment for psoriasis (Conlan & Sherman, 2001). A current clinical use of a $1,25(OH)_2D_3$ analog is the use of calcipotriene in the prescription cream Devonex, manufactured by Westwood Squibb, for the treatment of psoriasis. One of the most promising $1,25(OH)_2D_3$ discoveries is that $1,25(OH)_2D_3$ suppresses T lymphocytes, and may be useful as a therapeutic agent in procedures such as organ transplants (Lemire *et al*, 1992).

The human VDR gene was cloned and sequenced in 1988 by Baker *et al.*, and the protein sequence was predicted to be 427 amino acid residues. It is a member of a superfamily of structurally related nuclear receptors that function as transcription factors when bound to the appropriate hormone or ligand. Comparative studies of these receptors reveal a common structural organization, consisting of five homologous domains (Petkovich, Brand, Krust, & Chambon, 1987), shown in Figure 3. The gene encoding the VDR is located on chromosome 12cen-q12 (Taymans, Pack & Pak, 1999), contains 14 exons, and spans approximately 75 kilobases of DNA.

The ligand binding domain consists of 12 α-helices that fold in three layers, forming a hydrophobic binding pocket for the ligand. The C-terminal end of the ligand binding domain contains a subdomain required for transcriptional activation called AF-2. When the ligand binds, the ligand binding domain changes conformation, forming new surfaces,

including a hydrophobic cleft (Feng *et al.*, 1998). The three hydroxyl groups of $1,25(OH)_2D_3$ are thought to form hydrogen bonds with polar amino acid residues in the hydrophobic pocket of the VDR.

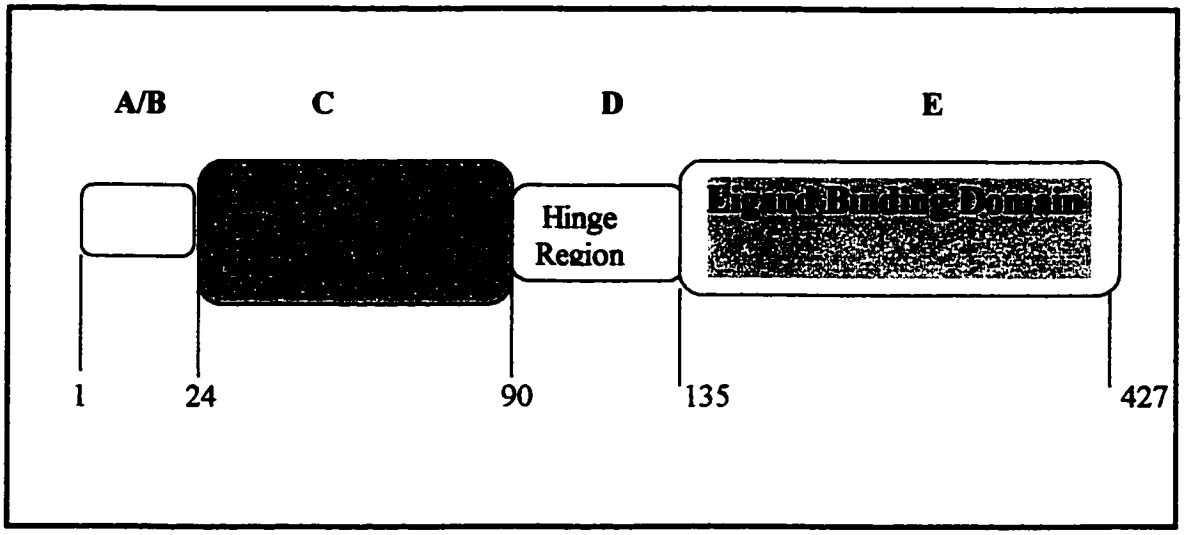

Figure 3- The Domain Structure of VDR. The A/B domain, residues 1-24 is the N-terminal domain. The C domain, residues 25-90, is the DNA binding domain. It contains two zinc finger domains. The D domain is the flexible hinge region. The E domain, residues 136-427 is the ligand binding domain. The E domain also contains a transactivation function (AF-2).

The X-ray crystallography structure of the ligand binding domain of VDR bound to $1,25(OH)_2D_3$ was recently determined (Rochel, Wurtz, Klaholz, & Moras, 2000). This crystal structure gives the most definitive information yet on the residues most likely to be in contact with the hydroxyl groups (see Table 1). The ligand binding domain was crystallized using residues 118-425, with a deletion of residues 165-215, in order to allow for the crystallization process. The x-ray crystallography structure indicated that the A-

ring of $1,25(OH)_2D_3$ was in the B-chair conformation, with the 3-OH group in the equatorial position (see Figure 4). Studies done from 1991-2001 indicate that mutations in several residues other than the residues identified as hydroxyl contact points in the crystal structure can have significant effects on ligand binding and transcription (Whitfield *et al.*, 1996, Jiménez-Lara & Aranda, 1999).

Table 1- Amino Acid Residues Involved in Hydrogen Binding to OH Groups of $1,25(OH)_2D_3$ (Rochel *et al.*, 2000)

Hydroxyl Group	**Hydrogen bonding to amino acid residues**
1-OH	237- Serine 274- Arginine
3-OH	143- Tyrosine 278- Serine
25-OH	305- Histidine 397- Histidine

Other research groups have proposed models of the ligand binding domain that have $1,25(OH)_2D_3$ docking in the A chair conformation, requiring other contact points for the three hydroxyl groups. NMR studies of $1,25(OH)_2D_3$ in solution (Okamura, Norman & Wing, 1974) have shown that either conformation of the A ring is possible, and that the A ring undergoes rapid interconversion between the two configurations. These models will be discussed in the literature review section.

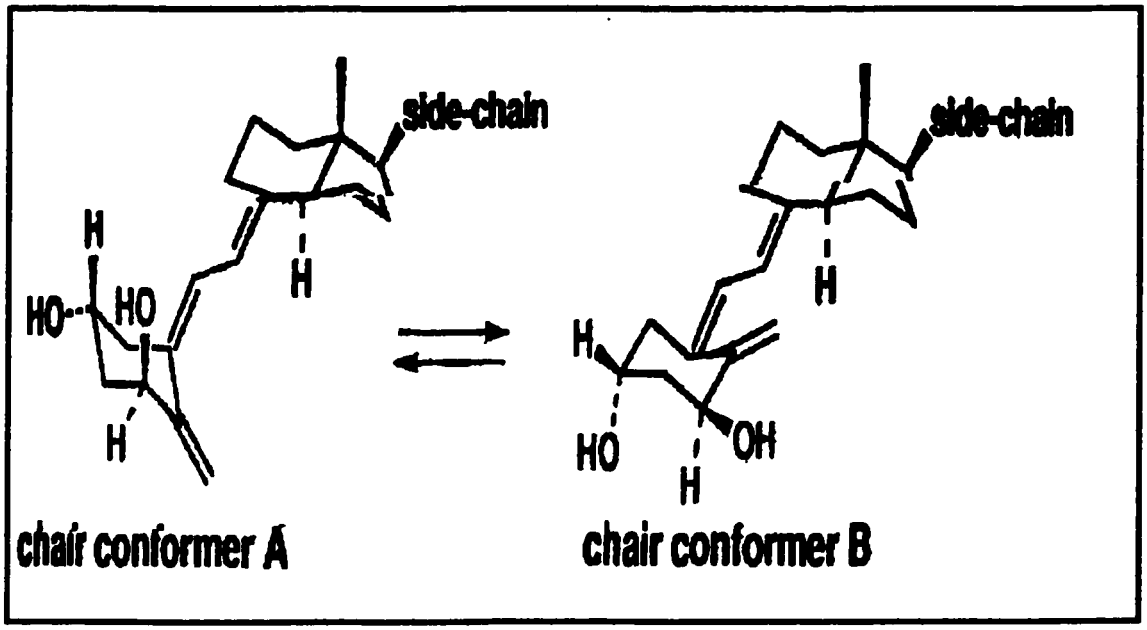

Figure 4- Ring Conformations of $1,25(OH)_2D_3$ (Collins & Norman, 2001)

Understanding how the vitamin D nuclear receptor binds the natural ligand is key to developing new analogs for therapeutic uses. The nuclear receptor is part of a complicated system that involves interactions with many other co-factors, and the biological effects induced by ligand binding are varied. The mechanisms of ligand binding and transcription effects induced by ligand binding need to be explored further to allow for future therapeutic developments. There are many future applications for drugs targeted to the nuclear receptor in the field of immunology, oncology, and skin disorders.

2.0 Literature Review

2.1 Categorization of Literature

The literature on ligand binding domain studies of the human vitamin D receptor can be divided into four categories: analog studies, site-directed mutagenesis studies, computer modeling studies, and crystallography studies. Analog studies focus on changes in conformation of VDR, biological activity, and binding affinity that occur when the structure of $1,25(OH)_2D_3$ is altered. Site-directed mutagenesis studies involve mutating one or more amino acid residues in VDR, and then evaluating how the binding affinity and/or the biological activity of $1,25(OH)_2D_3$ or an analog is changed. Computer modeling studies generate a model of VDR based on homology with a similar nuclear receptor. These studies then propose how $1,25(OH)_2D_3$ or an analog will bind. The X-ray crystallography structure for the ligand-binding domain of VDR bound to $1,25(OH)_2D_3$ has been determined and will be examined.

Analog studies have used a variety of $1,25(OH)_2D_3$ analogs, including F_6-$1,25(OH)_2D_3$ [26,26,26,27,27,27- hexafluoro–$1,25(OH)_2D_3$] and 20-epi-1,25-dihydroxyvitamin D_3 (Peleg *et al.*, 1995; Sasaki *et al.*, 1995; Väisänen, Juntunen, Itkonen, Vihko, & Mäenpää, 1997; Takeyama *et al.*, 1999). Binding-induced conformational changes to VDR have been determined in analog studies using trypsin and chymotrypsin digestion of the ligand-bound VDR, then analyzing the digestion fragment sizes generated compared to the natural ligand.

Binding affinity of analogs to VDR is often determined by using steroid competition binding assays. In these assays, increasing concentrations of $1,25(OH)_2D_3$ or an analog

are incubated with cell lysate containing VDR, in the presence of [^{3}H]-1,25$(OH)_2D_3$. The ability of each analog to compete with nonradioactive 1,25$(OH)_2D_3$ for receptor binding can be measured by the decrease in specific binding of [^{3}H]-1,25$(OH)_2D_3$ with increasing analog concentration. Specific binding is usually determined with a hydroxylapatite ($Ca_5(PO_4)_3OH$) batch assay, as described in section 4.11. The relative competitive index (RCI) is calculated by plotting the reciprocal of the percentage of maximum [^{3}H]-1,25$(OH)_2D_3$ bound on the ordinate versus [competitor]/[^{3}H]-1,25$(OH)_2D_3$] on the abscissa. The slope of the line obtained for an analog is divided by the slope of the line obtained for 1,25$(OH)_2D_3$, and then multiplied by 100. The RCI of 1,25$(OH)_2D_3$ is 100 by this calculation (Siebert, Ohnuma, & Norman, 1979).

Site-directed mutagenesis studies have been based on data indicating where mutations commonly occur in the VDR of vitamin D-resistant rickets patients, or from crystallography studies of VDR and other related nuclear receptors. Two natural VDR mutations have been determined to be R274L (arginine to leucine) by Kristjansson, Rut, Hewison, O'Riordan, & Hughes (1993) and H305Q (histidine to glutamine) by Malloy *et al.* (1997) in hereditary vitamin D resistant rickets. Prior to the publication of the X-ray crystallography structure of human VDR (Rochel *et al.*, 2000), the binding regions of VDR thought to be in closest contact with the natural ligand were residues 227-240, 268-316, and 396-422 (Haussler *et al.*, 1998). See appendix A for the complete 427 amino acid sequence of VDR (Baker *et al.*, 1988).

In site-directed mutagenesis studies, the mutation usually replaces a polar amino acid with a non-polar amino acid, or a hydrophobic residue with a hydrophilic residue. Next,

the mutant VDR must be produced and characterized. This is done in most studies by transfecting the mutated VDR cDNA (DNA that is complementary to the expressed VDR messenger RNA) into rat osteosarcoma (ROS) cells or monkey kidney cells (CV-1 or COS-7). The cells are then grown, and the cDNA translated into VDR protein. Saturation binding assays are used to evaluate the binding affinity of $1,25(OH)_2D_3$ to the mutated VDR. K_d, the dissociation equilibrium constant, is used in many studies as a measure of binding affinity. K_d is the ligand concentration at which half the binding sites are occupied. K_d is defined as:

$$K_d = [\text{Receptor}]^*[\text{Ligand}]/[\text{Receptor·Ligand}].$$

Defining a binding fraction, B, gives the relation $B=B_{max}^*[\text{Ligand}]/(K_d+[\text{Ligand}])$.

Both analog and site-directed studies may include the evaluation of transcriptional activity induced by ligand binding. VDR controls gene expression by dimerizing with retinoid X receptors (RXRs) producing heterodimers, and associating with vitamin D response elements (VDREs) in promoters of target genes (MacDonald *et al.*, 1993). VDREs have been identified in genes that are known to be transcriptionally regulated by $1,25(OH)_2D_3$. The VDREs used most frequently in recent studies are from human or rat osteocalcin gene, or the mouse osteopontin gene (Peleg *et al.*, 1995; Sasaki *et al.*, 1995; Whitfield *et al.*, 1996; Takeyama *et al.*, 1999). The osteocalcin and osteopontin genes are expressed in bone osteoblasts, cells that form new bone. The osteocalcin and osteopontin genes are both positively regulated by $1,25(OH)_2D_3$ binding, and their VDREs are defined as DR3s, or a direct repeat of two 6-base pair half elements, separated by a spacer of three nucleotides (Colnot, Lambert, Blin, Thomasset, & Perret, 1995; Nishikawa,

Kitaura, Matsumoto, Imagawa, & Nishihara, 1994). VDR occupies the 3' half site of positive DR3 VDREs, while the 5' half-site is bound by the RXR heteropartner (Jin & Pike, 1996). The nucleotide sequence of the osteocalcin and osteopontin VDRE (Haussler *et al.*, 1998) are shown in Table 2. Several studies use a consensus sequence for a VDRE compiled from many different genes.

This VDRE nucleotide sequence is attached to a reporter gene that encodes a protein that is easy to assay. Growth hormone gene and chlorampenicol acetyltransferase (CAT) genes are often used as reporter genes. Levels of the reporter protein are measured by radioimmunoassay or enzyme assay to determine the level of transcription that has occurred.

Table 2- VDRE Nucleotide Sequences in VDR-Regulated Genes

Gene	RXR Half Site	Spacer	VDR Half Site
Rat osteocalcin	GGGTGA	ATG	AGGACA
Human osteocalcin	GGGTGA	ACG	GGGGCA
Mouse osteopontin	GGTTCA	CGA	GGTTCA

2.2 Analog Studies

Analog studies use a modified chemical structure of $1,25(OH)_2D_3$ to investigate the structure-function relationship of the ligand, and the biological response to the ligand-VDR complex. Eliminating the hydroxyl group at C-1 or C-25 dramatically reduces binding, while eliminating the C-3 hydroxyl group reduces binding to a much lesser

degree (Bouillon, Okamura, & Norman, 1995). Modifying the 3-OH group to its epi conformer reduces binding as well, but does not eliminate it. This data would seem to indicate that the 3-OH group is less important for ligand binding compared to the 1-OH or 25-OH groups.

Many analog studies have focused on side chain modifications, as these analogs have shown the greatest biological impact on anti-proliferative activity. The transcriptional activity of F_6-1,25$(OH)_2D_3$ was studied by Sasaki *et al.* in 1995 using rat VDR and RXR. A CAT reporter gene with a consensus sequence VDRE was used to perform a transient transfection assay. The binding affinity was not evaluated in this study, as earlier studies of this analog had already determined that the analog binding affinity was slightly less than that of the natural ligand, 1,25$(OH)_2D_3$. Transcriptional activity was 2-4 times higher with the analog, indicating a significant change in the VDR conformation.

Peleg *et al.* performed a study in 1995, using two analogs: 20-epi-1,25-dihydroxyvitamin D_3, and 20-epi-22-oxa-24A, 26A, 27A-tri-homo-1,25-dihydroxyvitamin D_3. The 20-epi conformation orients the side chain over ring C, and induces a different VDR conformation, as determined by protease sensitivity studies. Binding affinities had previously been shown to be similar to 1,25$(OH)_2D_3$, but the antiproliferative action of the two analogs was shown to be 200 to 7,000-fold greater than that of 1,25$(OH)_2D_3$. This higher antiproliferative action was present without proportionally higher calcemic activity (Binderup *et al.*, 1991). This lack of higher calcemic activity is important for therapeutic applications, since using 1,25$(OH)_2D_3$ at equivalent doses results in too much calcium being present in the blood. The amount of

VDR binding directly to the osteopontin VDRE was also quantified using electrophoretic mobility shift assays. The analogs facilitated the DNA binding activity of VDR in a dose-dependent manner. More RXR dimerization with VDR was found with the two analogs, and trypsin digestion experiments indicated that the analogs induced a different conformational change in the VDR upon ligand binding compared to $1,25(OH)_2D_3$.

Väisänen, Juntunen, Itkonen, Vihko, and Mäenpää performed a study in 1997 comparing 20-epi-1,25-dihydroxyvitamin D_3 (MC1288), 20-epi-22-oxa-24a,26,27a-tri-homo-1,25-dihydroxyvitamin D_3 (KH1060), 1,25-dihydroxy-22,24-diene-24,26,27-tri-homo-vitamin D_3 (EB1089), and 1-(24S)-$(OH)_2$-22-ene-26,27-cyclopropyl vitamin D_3 (MC903) to $1,25(OH)_2D_3$. All of these analogs were previously known to have several orders of magnitude higher antiproliferative activity than $1,25(OH)_2D_3$ (Binderup *et al.*, 1993). In this study, no binding assays were done, but the comparison was made using trypsin and chymotrypsin digestion fragments. The digestion fragments of human VDR generated with the analogs KH1060 and MC1288 showed a greater protection of the VDR from digestion. This study concluded that the binding sites in VDR for the analogs do not differ detectably from those of the natural ligand, but that a different conformation in the VDR must be induced by the analog binding. These side-chain analog studies indicate that the ligand binding pocket can accommodate a large range of side chain conformations, and binding can still occur. While binding can still occur, the biological actions induced by the analog-VDR complex can be quite different those induced by the natural ligand-VDR complex.

2.3 Site-directed Mutagenesis Studies

Many studies have been performed using site-directed mutagenesis to determine which regions of VDR are important for ligand binding and which regions are involved in transcription activation. The C-terminal sequence between amino acids 390 and 427 has been identified as being essential for ligand binding activity as determined by mutational analysis and saturation binding analysis (McDonnell, Scott, Kerner, O'Malley, & Pike, 1989; Nakajima *et al.*, 1994), and was verified in a study performed by Lui, Collins, Norman and Peleg in 1997. In the Lui *et al.* study, deletion mutants were prepared in human VDR by inserting a stop codon at five different positions: residues 390, 396, 403, 410, and 420. A VDRE from human osteocalcin gene was attached to the growth hormone gene and used for transcription analysis. The transcriptional ability of $1,25(OH)_2D_3$ was abolished when residues 420-427 were deleted, and the ligand binding ability was decreased 50-70% (Figure 5). Ligand binding was evaluated using competition binding assays where each mutant VDR was incubated with $[^3H]$-$1,25(OH)_2D_3$ and increasing concentrations of unlabeled competitors. The maximal binding percentage is an average of three one-point assays. The free ligand was separated from bound by hydroxylapatite, and the amount of bound ligand quantified by liquid scintillation counting.

In this same study, point mutations of amino acids 420-422 and 425 were synthesized to determine which specific residues were important for binding the natural ligand. Glutamic acid at position 420 was replaced with alanine (E420A). The two hydrophobic

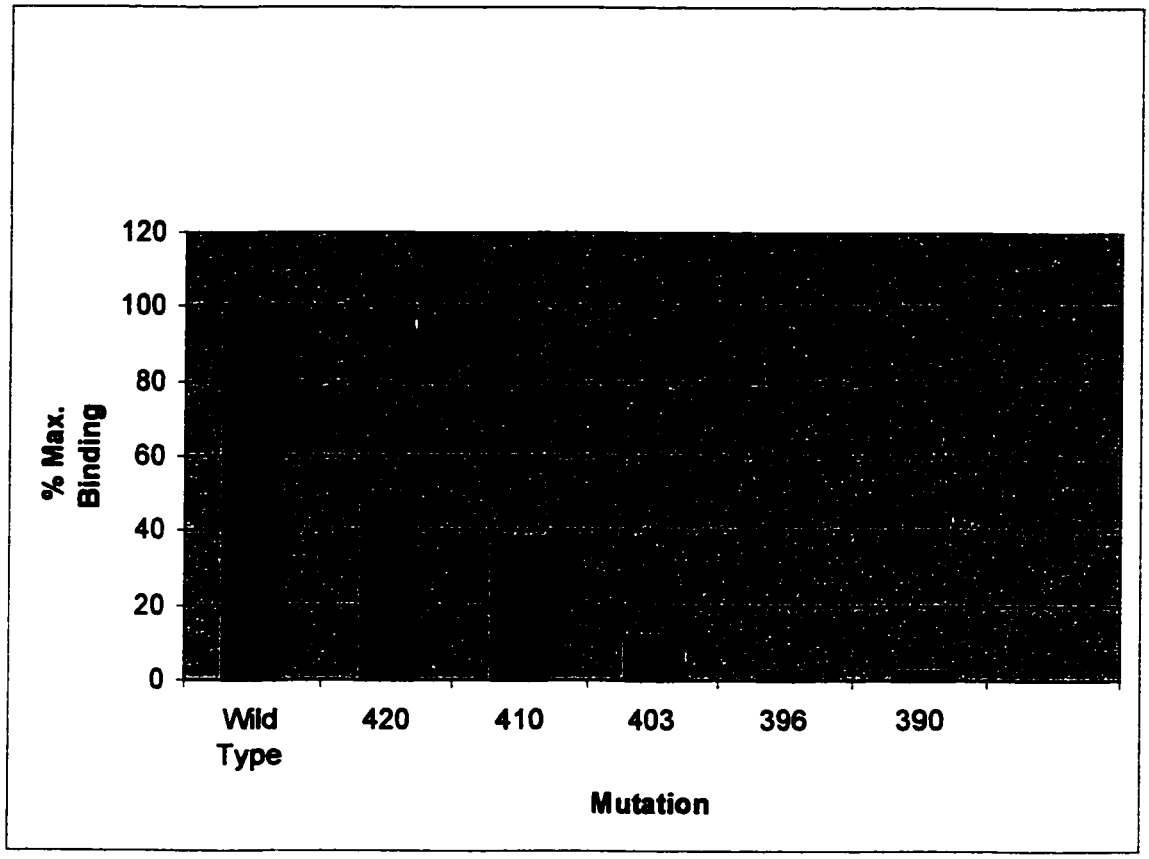

Figure 5- Percent Maximal Binding of $1,25(OH)_2D_3$ for Mutations in VDR. Mutation terminates VDR after the indicated residue (Lui *et al.*, 1997).

residues (valine at position 421 and phenylalanine at 422) were both mutated to methionine and alanine (V421M/F422A). At position 425, the glutamic acid was replaced with glutamine (E425Q). One-point saturation assays showed no change in the E425Q binding activity, but there was a significant decrease in ligand binding affinity for the double mutant V421M/F422A, to approximately 50% of wild type VDR. Mutant E420A also showed a significant decrease in the ability to bind $1,25(OH)_2D_3$ to

approximately 50% affinity of the wild type. Transcription was also severely decreased in E420A, and completely inactivated by V421M/F422A.

In 1995, Whitfield *et al.* examined another region of VDR, based on data identifying conserved regions with other nuclear receptors. Amino acids at positions 244-phenlyalanine, 246-lysine, 254-leucine, 259-glutamine, and 262-leucine were mutated separately to glycine. Binding assays were performed for each mutant, and the data plotted in the method of Scatchard to obtain an estimate of the dissociation constant K_d. The K_d value for wild type human VDR is approximately 0.10 nM. Each mutant was tested in two trials, and the results showed very similar K_d values, with the exception of F244G, which had a higher K_d in both trials. The data is shown in Table 3.

Table 3- K_d Data for $1,25(OH)_2D_3$ Binding with F244G, K246G,K246G, L254G, Q259G, L262G Mutated VDR (Whitfield *et al.*, 1995)

VDR Configuration	K_d- 1st trial	K_d- 2nd trial
Wild type	0.09 nM	0.11 nM
F244G	0.18 nM	0.18 nM
K246G	0.12 nM	0.12 nM
L254G	0.10 nM	0.17 nM
Q259G	0.07 nM	0.07 nM
L262G	0.11 nM	0.12 nM

Each mutant was tested for its ability to form a complex with rat osteocalcin VDRE using a gel mobility shift assay. Complexes were undetectable for F244G, L254G, and

L262G, while Q259G yielded a complex that was greatly reduced in intensity compared to wild type. The K246G mutant was able to form complexes that compared to wild-type VDR. The transcription activity was determined with a rat osteocalcin VDRE fused to a human growth hormone reporter gene. Transcription was dramatically reduced with all mutants using a 10^{-8} M $1,25(OH)_2D_3$ dose. A later study by Jiménez-Lara and Aranda in 1999 confirmed the transcription activity reduction for a similar mutant of position 246, using a lysine to alanine mutation.

A similar study in 1996 by Whitfield *et al.* investigated point mutations I314S (isoleucine to serine), and R391C (arginine to cysteine). These two mutations were both identified in the cDNA of patients with hereditary hypocalcemic vitamin D-resistant rickets. Two trials of saturation assays indicated that I314S had an average K_d value of 0.18 nM, and R391C had an average K_d of 0.08 nM, compared to the wild type average K_d of 0.10 nM. This data indicates that both mutants bind the ligand in the normal range.

Transactivation of the I131S mutant was impaired to approximately 20% of the wild type VDR, but it could be rescued to normal levels with higher doses of $1,25(OH)_2D_3$, up to 1 μM. The R391C mutant was also impaired with a transactivation ability of approximately 50% of the wild type and could also be rescued at the 1 μM dose of $1,25(OH)_2D_3$, although not to the same level as the I314S mutant.

Mutations in positions 288, 337, and 369 of the ligand binding domain were studied by Nakajima *et al.* in 1996. All three of these amino acid positions are cysteines in human VDR, and they were mutated to glycine. These cysteine residues are conserved between human, rat, and avian VDR receptors indicating that they may play an important role in

ligand binding (Baker *et al.*, 1988; Burmester, Wiese, Maeda, & DeLuca, 1988; Elaroussi, Prahl, & DeLuca, 1994). Only the mutation at position 288 showed a significant reduction in ligand binding affinity, using Scatchard analysis. The mutation at position 369 was equivalent to wild type binding affinity, and the position 337 mutation showed tighter binding. Data is shown in Table 4.

Table 4- K_d Data for $1,25(OH)_2D_3$ Binding with C288G, C337G, and C369G Mutated VDR (Nakajima, *et al.*, 1996)

Mutation	**Kd (pM)- summary of 4 trials**
Wild Type	86 +/- 15
C288G	292 +/- 40
C337G	25 +/- 7
C369G	77 +/- 2

The transcriptional activity of the mutants was evaluated with a rat osteocalcin VDRE fused to the growth hormone reporter gene. Mutant C288G did not show detectable transcription activation, C337G showed 60% of the wild type activation, and C369G was equivalent to the wild type. Increasing doses of $1,25(OH)_2D_3$ did bring the activation activity of C288G up to 100%, but required a $1,25(OH)_2D_3$ dose of 10^{-6} M.

The methods employed in performing site-directed mutagenesis studies are all very similar, and many studies of the same regions have been done. Table 5 summarizes the studies, including some studies not covered in detail in this section (See Appendix A for a

table defining the amino acid one-letter abbreviations). These studies show residues 229-234, 235, 237, 274, 275, 286, 288, 337, and 390-427 are important for normal ligand binding. Transcriptional activity is altered by changes to a much wider range of residues, and is completely abolished by the deletion of residues in the range of 390-420. This data indicates that ligand binding affinity does not predict transcriptional activity changes.

Table 5- Summary of Mutational Analysis of Ligand Binding Domain of VDR

Mutation	**Results**	**Reference**
C190W	Familial vitamin D-dependent rickets, type II	Thompson, Kristjansson, & Hughes, 1991
S208G	Phosphorylation that modulates transcription. Impaired transcription	Jurutka *et al.*, 1997
S225A	Slight impairment of transactivation, normal RXR dimerization	Kraichely, Collins, DeLisle, & MacDonald, 1999
S225A	Normal ligand binding	Väisänen, Rouvinen, & Mäepäneä, 1998
H229A	Impaired transactivation, reduced RXR dimerization, reduced ligand binding	Väisänen *et al.*, 1998 Kraichely *et al.*, 1999
D232A	Impaired transactivation, no RXR dimerization, reduced ligand binding	Väisänen *et al.*, 1998 Kraichely *et al.*, 1999
L233A	Abolished transactivation	Choi *et al.*, 2001
V234A	Reduced transactivation	Choi *et al.*, 2001
V234A	Slightly reduced binding	Väisänen *et al.*, 1998
S235A	Impaired transactivation, slightly reduced ligand binding	Väisänen *et al.*, 1998 Kraichely *et al.*, 1999
Y236A	Normal ligand binding, normal RXR dimerization, impaired transactivation	Kraichely *et al.*, 1999

Mutation	Results	Reference
S237A	Reduced transactivation	Choi *et al.*, 2001
S237A	Impaired ligand binding	Väisänen *et al.*, 1998; Collins & Norman, 2000
K240A	Slight impairment of transactivation, normal RXR dimerization, slightly reduced ligand binding	Väisänen *et al.*, 1998 Kraichely *et al.*, 1999
I242A	Normal ligand binding	Väisänen *et al.*, 1998
F244G	Impaired transactivation, no RXR dimers	Whitfield *et al*, 1995
K246A	Reduced ligand binding Impaired transactivation	Whitfield *et al*, 1995 Jiménez-Lara & Aranda, 1999
K246G	Impaired transactivation	Whitfield *et al.*, 1995
L254G L262G	Impaired transactivation, no RXR heterodimers	Whitfield *et al.*, 1995
R274A	Reduced transactivation	Choi *et al.*, 2001
R274A	Reduced ligand binding	Väisänen *et al.*, 1999
R274L	Reduced ligand binding	Thompson *et al.*, 1991
S275A	Reduced transactivation	Choi *et al.*, 2001
S275A	Reduced ligand binding	Väisänen *et al.*, 1998
S278A	Little affect on transactivation	Choi *et al.*, 2001
W286A	No transactivation	Choi *et al.*, 2001
W286A	No ligand binding	Solomon *et al.*, 2001
C288G	Familial vitamin D-dependent rickets, type II. Reduced ligand binding	Nakajima *et al.*, 1996
C288A	Reduced transactivation	Choi *et al.*, 2001
Y295-stop	Premature termination, no ligand binding	Ritchie *et al.*, 1989
H305A	Reduced transactivation	Choi *et al.*, 2001
I314S	Impaired transactivation and RXR dimerization	Whitfield *et al.*, 1996
C337G	Reduced ligand binding	Nakajima *et al.*, 1996

Mutation	Results	Reference
C369G	Impaired transactivation, no RXR dimerization	Whitfield *et al.*, 1996
M383G/Q385A	Reduced dimerization	Lui, Nguyen, & Peleg, 2000
L390-stop E396-stop	No binding, no transactivation	Lui *et al.*, 1997
R391C	Impaired transactivation, no RXR dimerization	Whitfield *et al.*, 1996
H397A	No transactivation	Choi *et al.*, 2001
Q400A	No transactivation	Choi *et al.*, 2001
Y401F	No change in binding	Collins & Norman, 2000
Y401A	No transactivation	Collins & Norman, 2000; Choi *et al.*, 2001
C403-stop	Severely reduced binding, no transactivation	Lui *et al.*, 1997
C410-stop	Reduced binding, no transactivation	Lui *et al.*, 1997
L417S	Impaired transactivation	Jiménez-Lara & Aranda, 1999
L417A E420A	Impaired transactivation	Jurutka *et al.*, 1997
E420-stop	Reduced binding, no transactivation	Lui *et al.*, 1997
E420Q	Impaired transactivation	Jiménez-Lara & Aranda, 1999

2.4 Crystallography Data of VDR

An X-ray crystallography study published in 2000 (Rochel, Wurtz, Klaholz, & Moras, 2000) added new information to the data on VDR. The X-ray crystallography study was done on VDR ligand binding domain (residues 118-425) with a deletion of residues 165-215. Sequence comparisons had shown this deleted region to be highly variable between different VDR species, and no known biological significance has yet been determined for this region. This deleted region contains a high percentage of

negatively charged residues and is predicted to have only a few short β strands as secondary structure. These factors were thought to increase the number of conformers, affecting protein stability and interfering with the crystallization process. The ability of the mutant VDR (residues 118-425, Δ [165-215]) to bind $1,25(OH)_2D_3$ and analogs was compared to the ability of wild type VDR and found to be similar. Transactivation properties of VDR with the deletion and wild type VDR were also compared and found to be similar.

In the crystal structure, helix 1 of the ligand binding domain was determined to be comprised of residues 125-142 and a small helix 2 was comprised of residues 149-153. Since residues 165-215 were deleted, the truncated loop between helix 1 and helix 3 consists only of residues 154-164 and a small helix 3n of residues 216-223. Helix 3 is comprised of residues 225-246. In the crystal structure, the truncated loop between helix 2 and helix 3n runs straight down between helix 2 and the β-strands, like the estrogen and progesterone receptors which belong to a different subfamily of nuclear receptors than VDR. In the crystal structures of nuclear receptors in the same subfamily as VDR (retinoic acid receptor, thyroid receptor, and peroxisome proliferator activated receptor) this loop instead goes around the β-strands (Choi, Yamamoto, Masuno, Nakashima, Taga, & Yamada, 2001).

The crystal structure data shows the A ring of $1,25(OH)_2D_3$ to be docked in the B-chair conformation. The ligand binding pocket was found to be lined with predominately with hydrophobic residues, and the specific residues that contact the ligand hydroxyl groups were serine-237, arginine-274, serine-278, tyrosine-143, histidine-305, and

histidine-397, as shown earlier in Table 1. This data was surprising, in that it showed residues 143 and 278 involved in H-bonding interactions with the 3-OH group, positions that had not yet been the subject of site-directed mutagenesis studies. Other studies on residues 237 and 274 had shown impaired ligand binding when mutations were introduced (Thompson *et al.*, 1991; Väisänen *et al.* 1998; Collins & Norman, 2000). Residue 305 did show a slight decrease in ligand binding when mutated, and residue 397 showed a severe decrease in binding affinity when deleted with residues 397-427 in the Lui *et al.* study of 1997.

2.5 Models of VDR

Before the crystal structure of the ligand binding domain of VDR was determined, several computer models were developed. One computer model was reported (Yamamoto *et al.*, 1999) based on the retinoic acid receptor crystal structure, eliminating residues Y143-Q223 in loop 1-3, assuming them to be insignificant to the 3-D structure of the ligand-binding pocket. The Yamamoto *et al.* model is almost identical to the crystal structure in its assignment of residues to helix 1. The Yamamoto *et al.* model assigns residues 124-142 to helix 1; in the crystal structure helix 1 is comprised of residues 125-142. Helix 3 is comprised of residues 225-247, and helix 2 is not identified. This helix 3 residue assignment is almost identical to the crystal structure assignment of residues 225-246 to helix 3. This model is compared to the crystal structure in Figure 6.

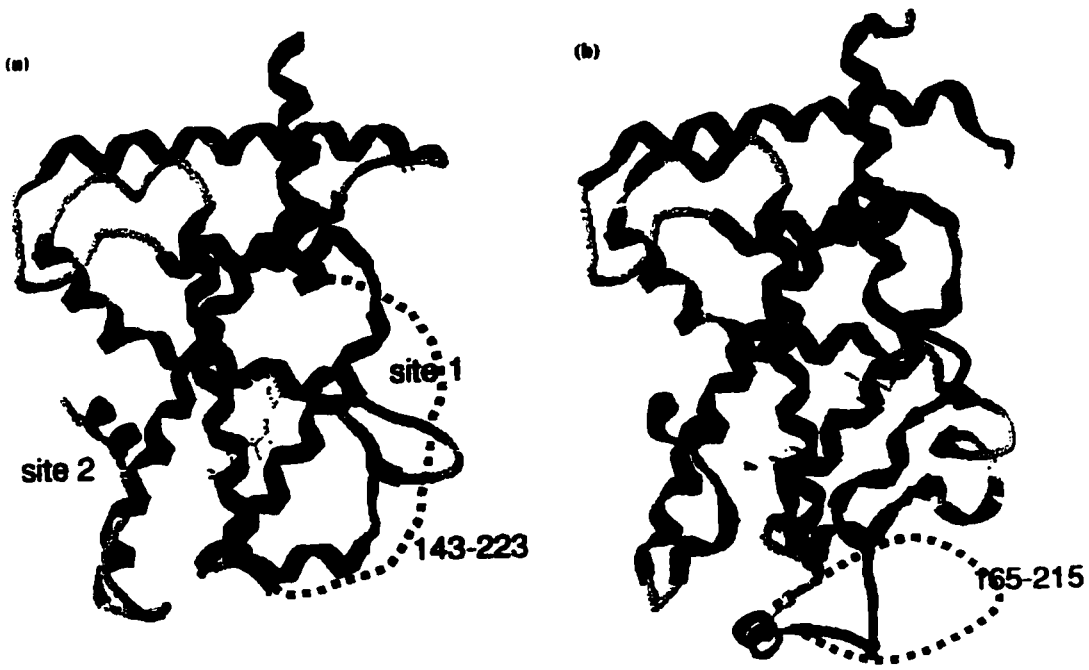

Figure 6- Comparing Models of the Ligand Binding Domain
(a) Yamamoto *et al.* model of the ligand binding domain. Residues Y143-Q223 are eliminated, and represented by the blue dotted line. Site 1 is the A-ring anchor position, site 2 is the side-chain anchor position. A ring is in the A chair conformation
(b) Crystal structure of the ligand binding domain, with residues S165-P215 deleted. They are represented by the blue line. A ring is in the B chair conformation.
Ribbons represent a- helices and B-sheets, tubes represent loops. The ligand is shown in gray docked to the ligand binding domain (M.Choi *et al.*, 2001).

One key feature of the Yamamoto *et al.* model is its prediction that the ligand docks in the A chair conformation of the A ring, whereas it docks in the B-form in the crystal

structure. The Yamamoto *et al.* model predicts hydrogen bonding to the hydroxyl groups of $1,25(OH)_2 D_3$ at residues 237 and 274 for the 1-OH group, residue 288 for the 3-OH group, and residue 397 for the 25-OH group. Residue 288, predicted to be the hydrogen bond for the 3-OH of the hormone is assigned to the region between helix 5 and 6. The 143 residue cited as a contact point in the crystal study was deleted from the Yamamoto *et al.* model, as Y143 is not conserved in all species and was assumed to be non-essential in ligand binding.

The Yamamoto *et al.* study evaluated twelve mutants based on their model and conservation of residues between species. In this study, C288 was predicted to be in contact with the 3-OH group of the ligand rather than S278 as predicted in the crystal structure. A luciferase reporter assay was used to determine transcriptional activity, and the mutants L233A, R274A, W286A, H397A, and Y401A abolished transcriptional activity. Mutants V234A, S237A, S275A, C288A, and H305A moderately reduced activity, while S278A and Q400A had little affect. Residue C288 was altered in the Nakajima study of 1996 (Table 4) to glycine and also found to reduce binding affinity of the ligand.

A different model of the VDR ligand binding domain (Norman, Adams, Collins, Okamura, & Fletterick, 1999) was published the same year. This model aligned the residues 142-427 of VDR to residues 157-410 of the rat α1 isoform of the thyroid receptor. In the Norman *et al.* model, helix 1 is comprised of residues 147-161, helix 2 of residues 172-175, and helix 3 of residues 225-249. This model has two proline residues

(155,156) in helix 1, that are not normally found in α-helices. The authors suggest that helix 1 will be nonlinear due to these two proline residues.

The Norman *et al.* model differs from the X-ray crystallography data in the alignments of helix 1,2, and 3, and has no small helix 3n. Helix 1 begins further downstream, and is comprised of residues 147-161. This model places residue 143 outside the ligand binding pocket so it cannot be a hydrogen bond donor for any hydroxyl group. Helix 2 is comprised of residues 172-175, resulting in a small four-residue helix that is similar in size to the small helix 2 in the crystal structure. The residues comprising helix 3 are almost identical in the Norman *et al.* model and the crystal structure, with the Norman *et al.* model helix 3 comprised of residues 225-249 and the crystal structure helix 3 is comprised of residues 225-246. The loop between helix 1 and helix 3 in the Norman *et al.* model includes helix 2, and consists of residues 161-225, which is a shorter loop than suggested by the crystal structure.

The Norman *et al.* model predicts that the B-*trans* ($1,25(OH)_2$-6-s-*trans* D_3) conformer or the A-*cis* conformer can be docked, but that the plane of the A-ring in relation to the C/D ring is at an angle between 0-90°, due to the lack of biological activity of *cis*-locked or *trans*-locked analogs. In this model the ligand binding domain volume is predicted to be large enough to accommodate either the A or B chair conformation of the A ring of $1,25(OH)_2D_3$.

In the Norman *et al.* model, residues S235 and S237 are close enough to the 1-OH group to form hydrogen bonding interactions. The 3-OH group of docked $1,25(OH)_2 D_3$ is close enough to the S275 residue of VDR to form hydrogen bonding interactions, and

residues H305, S306, Y401, and S405 are in proximity to the ligand for hydrogen bonding with the 25-OH group.

The S275 residue, predicted by the Norman model to be in hydrogen bonding proximity to the 3-OH group, was mutated to alanine, and K_d reported as 5.29 +/- 0.09 nM (Väisänen *et al.*, 1998) compared to wild type K_d 1.02 +/- 0.02 nM. This data seems to support the Norman *et al.* model prediction. Mutation of Y401, predicted by the Norman *et al.* model to be in hydrogen bonding proximity to the 25-OH group, to phenylalanine indicated no significant change in binding affinity: K_d=0.84 +/- 0.54 nM compared to wild type K_d=0.67 +/- 0.18 nM (Collins & Norman, 2000). This data suggests that the predicition of Y401 as a hydrogen bond donor may not be correct.

Residue S237 is predicted by both models and the crystal structure as a hydrogen bonding residue for 1-OH, and does result in reduced binding when modified to alanine. K_d for S237A was reported as 23.29 +/- 0.16 nM compared to 1.02 +/- 0.02 nM for wild type by Väisänen *et al.* (1998). Collins and Norman (2000) reported a K_d value of 1.5 +/- 0.34 nM for S237A compared to 0.67 +/- 0.18 nM for wild type VDR. While these values differ widely, they both indicate that modifying S237 does result in reduced binding, and that S237 may be involved in hydrogen bonding to the 1-OH group. S237 is located in helix 3 in both models and the crystal structure.

The Yamamoto *et al.* and Norman *et al.* models are compared to the X-ray crystallography data in Table 6. The key differences between the models and the X-ray crystallography data are the amino acid residues that comprise helix 1, and the number of residues in the loop between helix 1 and 3.

Table 6- Comparison of VDR X-ray Crystallography Data and VDR Models

VDR Structure	X-ray Crystallography Data Rochel *et al.*, 2000	Norman *et al.*, 1999, Model	Yamamoto *et al.*, 1999, Model
Helix 1 residues	125-142	147-161	124-142
Loop between Helix 1 and 3 residues (includes helix 2)	154-164, 216-223	161-224	143-224
Helix 2 residues	149-153	172-175	none
Helix 3 residues	225-246	225-249	225-247

2.6 Summary of Literature Review

The literature review shows a wide range of studies of vitamin D nuclear receptor mutants, $1,25(OH)_2D_3$ analog studies, VDR crystallography data and modeling of VDR. However, some of the data is contradictory, and further research is necessary. The Choi *et al.* study of 2001 discounts the importance of residues 143 and 278 as contact points for the 3-hydroxyl group, although these residues are in contact with the 3-OH group in the crystal structure. The effect of mutation S278A on binding was reported (Yamamoto *et al.*, 1999) as slightly reducing binding affinity, but K_d values were not reported. Residue 143 has not been mutated in any studies to date. The 143rd residue is predicted to be outside the ligand binding pocket by two modeling studies, so its involvement in the binding of the 3-OH group of $1,25(OH)_2D_3$ is an area worthy of further study. In

addition, further study of the S278A residue is warranted to further characterize the binding affinity of $1,25(OH)_2D_3$ to the mutant VDR.

3.0 Research Hypothesis and Objective

3.1 Research Hypothesis

The hypothesis underlying this research is that altering amino acid residues 143 and 278 in the human vitamin D receptor will significantly change the binding affinity of $1,25(OH)_2D_3$, based on crystallography data.

3.2 Research Objective

The research objective is to determine binding constants of three mutants of human vitamin D receptor, based on the X-ray crystallography data of Rochel *et al.*, which identifies amino acids at positions 143 and 278 as contact points for the 3-0H group of $1,25(OH)_2D_3$. In order to accomplish this goal, three mutant VDRs will be constructed using site-directed mutagenesis: Y143F (tyrosine to phenylalanine), S278A (serine to alanine), and the double mutant (Y143F-S278A). These mutants will be sequenced to verify that only the desired mutation is present. The binding affinity of these mutants to $1,25(OH)_2D_3$ will be characterized by performing saturation binding analysis. The questions to be answered by this research are:

1. Does mutating either of these vitamin D nuclear receptor polar amino acids to a non-polar amino acid change the binding constant for $1,25(OH)_2D_3$? If these amino acids are actually in contact with the 3-OH group of $1,25(OH)_2D_3$ there should be significant reduction in binding affinity.

2. Does mutating both amino acids at the same time have an additive effect on binding affinity? Do both residues make an equal contribution, and if not, what contribution do they make? If one mutation reduces binding significantly more than the other, then that residue may be a larger contributor to binding than the other. If the mutations reduce binding affinity by the same amount, then they can be considered to be equal contributors to hydrogen bonding.

4.0 Methods and Materials

4.1 Buffers and Solutions

Ampicillin Solution: 100 μg/ μL (Ampicillin Sodium Salt- 941.3 μg/ mg, Mediatech)

Chloraquine Solution: 8 mM

DEAE 1X Solution: 1 g DEAE-dextran hydrochloride per 100 mL phosphate buffered Saline (10 mM). Filter sterilize using 0.22 μM filter.

DMEM Media Solution: Dulbecco's modified Eagle's medium with 1.5g/L sodium Bicarbonate (Mediatech #50-013-PC) , 10 mL/L antibiotic solution (Cellgro 3C-004-C1 100X: 10,000 U/mL Penicillin, 25 μg/mL amphotericin, 10,000 μg/mL streptomycin), 10% fetal calf serum.

DMEM Media with 80 μM chloraquine: 10 μL of 8 mM chloraquine solution per 1 mL DMEM media solution.

NZY+ Broth: 11 g NZCYM powder (Difco) per 490 mL DI water,
12 mM $MgCl_2$, 0.02 M glucose. Filter sterilize using 0.22 μM filter.

TBE 1x buffer: 89 mM Tris, 89 mM Boric acid, 2 mM EDTA (Trisodium Ethylenediaminetetraacetate Trihydrate)

TED buffer: 10 mM Tris-HCl, 1 mM EDTA, and 0.5 mM DTT (Dithiothreitol), pH 7.5

TED/Triton Buffer: 0.5% by volume Triton-100X in TED buffer.

4.2 Site-directed Mutagenesis

The cDNA of wild-type VDR was cloned into a plasmid (pcDNA1.1/Amp, Invitrogen, CA) containing an ampicillin-resistance gene, using the Eco R1 and Nsi I sites. The Eco R1 site was added to the cDNA of the wild type VDR before the Alanine-3 position during the original cloning of the VDR from a human intestinal cDNA library (Baker *et al.*, 1988). See Appendix B for the pcDNA1.1/Amp map. Site-directed mutagenesis was performed on this plasmid using the Quik-Change Kit (Stratagene, CA). The site-directed

mutagenesis process was optimized to use the following conditions: 10 ng template DNA, 125 ng each of mutant primers (forward and reverse), 5 μL10X reaction buffer (Stratagene), 34.84 μL nuclease-free water, 1.0 μL dNTP mix, and 1.0 μL Turbo Pfu-DNA polymerase enzyme (2.5 U/μL). Primers used are listed in Table 7.

Table 7- Primers Used for Site-Directed Mutagenesis and Sequencing
Codon change is in bold

Primer	**Sequence**
S278A forward primer	5'-CGCTCCAATGAG**GCC**TTCACCATGG-3'
S278A reverse primer	5'-CCATGGTGAA**GGC**CTCATTGGAGCG-3'
Y143F forward primer	5'-CCATAAGACC**TTC**GACCCCACCTAC- 3'
Y143F reverse primer	5'-GTAGGTGGGGTCG**AAG**GTCTTATGG- 3'
T7-sequencing	5'-TAATACGACTCACTATAGGG-3'
305-sequencing	5'-GCATCACCAAGGACA-3'
479-sequencing	5'-CCCAAGCTGTCTGAGG-3'
502-sequencing	5'-AGCGCATCATTGCCATA-3'
824-sequencing	5'-GGTCATTGGCTTTGC-3'
935-sequencing	5'-GCGCTCCAAGTCCTT-3'
1164-sequencing	5'-GCTGATTGAGGCCAT-3'

This mixture was then heat cycled using an MJ Research Minicycler for 30 seconds at 95°C, 25 cycles of 30 seconds at 95°C, 1 minute at 55°C, and 12 minutes at 68°C,

followed by a hold step at 4°C. Following the heat cycling, 1 U of DPN I restriction enzyme (Stratagene) was added to the site-directed mutagenesis mixture, and the mixture incubated for 1 hour at 37°C.

4.3 Bacterial Cell Transformation

Epicurian *E. Coli* XL-1 Blue supercompetant cells (Strategene) were transformed with the site-directed mutagenesis DNA. Falcon 2059 tubes were prechilled on ice for 15 minutes before adding 50 μL XL-1 cells. Either 1 μL or 4 μL of the site-directed cfacmutagenesis DNA was added, and the cell mixture was incubated on ice for 30 minutes. The cells were heat-shocked at 42°C for 45 seconds, in a Precision 183 water bath. NZY+ broth, preheated to 42°C, was added (0.5 mL), and the mixture incubated for one hour at 37°C in a Lab-line Orbit Environ Shaker shaking incubator at 225 rpm. Following incubation, the entire solution volume was spread on a LB agar-ampicillin plate (100 μg ampicllin /mL LB agar). The plates were incubated in a 37°C Thermodyne Type 37900 Culture Incubator for 16-40 hours. Positive colonies were selected at the end of this incubation period, and up to ten colonies were regrown on a LB agar-amplicillin master plate to confirm the presence of the ampicillin-resistance containing plasmid.

4.4 Plasmid Mini-preparations

Overnight cultures were grown of the bacterial colonies from the master plates. For each overnight culture, 3 mL of NZY+ broth with 100 μg/mL of ampicillin was placed into a culture tube. Colonies were transferred into the broth using a sterilized wood stick.

The culture tubes were then incubated 16-20 hours in the shaking incubator at 37°C with shaking at 250 rpm. An Eppendorf Perfect Prep Mini kit was then used to purify the plasmid, following the kit directions. The final step was to resuspend the DNA in 10 μL of nuclease-free water.

4.5 Restriction Digest

A 5 μL sample of the plasmid prep was digested with 1 μL EcoR1 restriction enzyme (Promega- 12 U/μL), 1μL 10X EcoR1 buffer (Promega), and 3 μL nuclease-free water for 1 hour at 37°C. The presence of a DNA plasmid of the correct base pair size was verified using a 1% agarose gel in 1X TBE buffer. An aliquot of 5 mg/mL ethidium bromide (2.5 μL) solution was added to the gel solution, before it was poured into a Fisher Scientific FB-SB-710 gel apparatus and allowed to set for 45 minutes. The DNA samples were prepared by adding 2 μL of blue-orange loading dye (Promega) to each 10 μL digestion sample. A marker standard was prepared to run with the DNA samples consisting of 2 μL blue-orange loading dye, 1 μL of 0.50 μg/mL Hind III/ Eco RI cut Lambda Markers (Promega), and 9 μL 1X TBE buffer.

A 10 μL aliquot of each DNA sample and the marker was loaded into the gel, and electrophoresed at 120 volts for 70 minutes, using 1X TBE buffer as the conducting buffer in the Fisher Scientific FB-SB-710 gel apparatus. The completed gel was visualized using the Strategene Eagle-Eye Jr. System with version 3.2 Eagle Eye software.

4.6 DNA Sequencing

Dideoxy sequencing of positive colonies was performed using a Promega fmole sequencing kit, and Novex SureLock gel apparatus. The primers for dideoxy sequencing were complementary to DNA approximately 100 bp upstream of the desired mutation location in the cDNA. See Table 7 for the sequencing primers used. Each primer was labeled with γ-[^{33}P]- ATP by mixing 1 μL of primer solution (100 pmol/μL), 10 pmol γ-[^{33}P]- labeled ATP- (Amersham Pharmaceuticals-2500 Ci/mmole specific activity), 1 μL 10X T4 Polynucleotide kinase buffer, 0.50 μL T4 Polynucleotide kinase enzyme (10U/ μL), and 5 μL nuclease-free water. This solution was incubated for 30 minutes at 37°C, then 90°C for 2 minutes. When the primer labeling reaction was completed, the dideoxy sequencing reaction mixtures were prepared by mixing 5 μL of the DNA plasmid mini-prep, 5 μL of 5X sequencing buffer, 4.5 μL nuclease-free water, 1.5 μL ^{33}P-labeled primer, and 1 μL Taq polymerase (5U/μL). Four tubes, each containing one dideoxynucleotide (G, A, T, or C) were prepared for each plasmid prep, with 2 μL of the appropriate deoxy/didexoy nucleotide solution from the fmol sequencing kit. The sequencing reaction mixture (4 μL) was then added to each of the four nucleotide tubes for each plasmid prep. The tubes were then heat-cycled using the MJ Research Minicycler preheated to 95°. The heat cycle used was 2 minutes at 95°C, then 30 cycles of 30 seconds at 95°C, 30 seconds at 42°C, and 1 minute at 70°C, followed by a 4°C hold.

Upon completion of the sequencing reactions, the samples were run on the Novex SureLock sequencing gel, using the kit directions. Samples of the dideoxy reaction mixtures (0.5 μL) were electrophoresed for 8 minutes at 1200 volts. The gel was then

fixed in 10% acetic acid solution for 10 minutes, rinsed in distilled water for 10 minutes, and dried in the microwave at 50% power for 4.0 minutes.

The dried gel was then placed with Kodak Biomax Autoradiography film in a darkroom, enclosed in a lightproof cassette, and allowed to expose for 3-7 days. When the exposure was completed, the film was transported to the SJSU Student Health Center, where it was developed using the Kodak RP-X –Omat Model M-7B Processor. The film was then read manually.

Some sequencing reactions were run on another gel system, using a large 6% urea-polyacrylamide sequencing gel. The gel was made with 60 mL Sequa-Gel-6 solution (National Diagnostics), 15 mL Sequagel Complete Buffer, and 300 μL 10% ammonium persulfate. The large polyacrylamide gel was run for 90 minutes at 70 watts constant power. The gel was dried in a Savant gel dryer, and then exposed to Kodak Biomax film for 3-7 days, developed, and read manually.

Clones positive for mutations were selected, and large-scale plasmid preparations were made of the mutants. The entire DNA sequence of each mutant VDR was verified at the UC Davis sequencing facility or by manual sequencing. See Appendix C for the sequencing data.

4.7 Large Plasmid Prep

Plasmids for the three mutants were grown in larger quantity, using 100 ml of LB broth in each of two 250 ml culture flasks, with 100 μL ampicillin solution added to each flask. An overnight NZY+ culture of the bacterial colony containing the appropriate

mutant cDNA (500 μL) was added to each flask. The 100 mL cultures were grown overnight in the shaking incubator at 37°C, at 250 rpm. The 100 ml overnight cultures were combined, and the plasmid purified using a Qiagen Maxi-Prep kit.

4.8 Cell Culture

African green monkey COS–1 cells (ceropcithecus aethiops kidney) were obtained from American Type Culture Collection (ATCC, Rockville, MD). Cells were maintained in continuous culture in Dulbecco's modification of Eagle's medium (Cellgro) supplemented with 10% fetal calf serum (Sigma), 1.5 g/L sodium bicarbonate, and 1% Antibiotic-Antimycotic (Cellgro) in a Forma Scientific 37900 incubator at 37°C in a 92% humidified atmosphere of 95% air, 5% CO_2. Cells were subcultured every 3-4 days at 90-100% confluence.

4.9 Transfection of COS-1 Cells

Transfection of the DNA into COS-1 cells was done using DEAE-Dextran assisted transfection (McCutchan and Pagano, 1968), using six 100mm dishes of COS-1 cells grown to 70-80% confluence. DNA was ethanol precipitated using 18.9 μg of DNA, two volumes of absolute ethanol, and one-tenth volume of 5 M NaCl. This mixture was then placed in a –70° C freezer for 20 minutes, centrifuged at 4°C for 15 minutes at 13,000 x g, and the supernatant removed under sterile conditions. The pellet was allowed to air dry, then resuspended in 3.8 mL of PBS buffer.

Media was removed from the cells by aspiration and cells were washed with 10 mL of PBS buffer per dish for 15 minutes at room temperature. The PBS buffer was aspirated from the dishes, and 4 mL of 10% DEAE-Dextran solution was added to each dish for exactly 9 minutes. The 10% DEAE-Dextran solution was removed, and cells were washed with 5 mL of PBS buffer. After removal of PBS, 0.60 mL of the plasmid DNA/PBS solution was added to each dish. The dishes were placed in the cell culture incubator for 30 minutes, with the dishes being rocked every 10 minutes to evenly distribute the DNA solution. At the conclusion of the incubation period, 6 mL of media with chloraquine was added to each dish. After 3-4 hours had elapsed, the chloraquine media was removed, and 8 mL of new media without chloraquine was added to each dish. Dishes were then allowed to incubate for 68-72 hours.

4.10 Harvesting of COS-1 Cells

The 6 dishes of COS-1 cells were harvested with Trypsin-EDTA after the incubation period and resuspended in 3.2 mL of TED buffer. The cells were homogenized by aspiration five times through a 20-gauge needle syringe, and the cell lysate put on ice.

4.11 Binding Assays

Aliquots of cell lysate (100 μL) were incubated with 10 μL aliquots of varying concentrations of [^{3}H]-1,25(OH)$_2$ D$_3$ in ethanol, in the presence or absence of excess non-radioactive 1α,25(OH)$_2$ D$_3$. Six different concentrations of [^{3}H]-1,25(OH)$_2$ D$_3$ were used, with 5 incubation tubes at each concentration: 3 without any excess unlabeled 1,25(OH)$_2$ D$_3$, and 2 tubes with 100 times excess unlabeled 1,25(OH)$_2$ D$_3$. The choice of

concentrations was based on the physiological concentration of $1,25(OH)_2 D_3$ in the range of 1 nM (Makin, Lohnes, Byford, Ray & Jones, 1989). The cell lysate was incubated with the $[^3H]$-$1,25(OH)_2 D_3$ solution for four hours at 4°C. A 50 % slurry of hydroxylapatite and TED buffer (300 µL) was added to each tube at the end of the incubation period. The tubes were vortexed, and the hydroxylapatite washed three times with 1 mL of TED-0.5% Triton X-100 by centrifugation at 2245 x g for 1 minute. The final pellet was extracted with 1 mL of absolute ethanol. The ethanol was decanted into scintillation vials for liquid scintillation counting. Ecoscint scintillation fluid (3 mL) (National Diagnostics) was added to each vial. Vials were counted on the Beckman LS6500 scintillation counter, using the program listed in Table 8.

Table 8- Beckman LS6500 Scintillation Counter Settings for Binding Assay Measurements

Parameter	Setting
Time per sample	2.0 minutes
Isotope 1	3H
Isotope 2	None
Replicates	1
Repeats	1
Cycle Reps	1
Low Reject Threshold Level	0 cpm
Counting Precision (% 2 sigma)	2.0
Background Subtract	None
Quench Monitor	H #
Calculation Mode	SL DPM
AQC	Off
Lum-Ex Correction	No

5.0 Results

5.1 Site-directed Mutagenesis and Sequencing

The site-directed mutagenesis process for all mutants required several trials at different heat cycle conditions and an increase in primer concentration, due to a high degree of secondary structure of the primers. Once positive clones were identified, the mini plasmid purification of mutated DNA was also difficult. The yield of plasmid from the purification protocol was poor, resulting in difficulty with sequencing. The sequencing process was repeated several times using the 824 primer in order to get a readable gel image and several more times in order to find a mutated DNA sequence for the 278 mutant. The mutated sequence for 278 is shown in Figure 7.

The 143 residue mutant was verified after multiple mini plasmid preparations were pooled in order to accumulate 100 ng of DNA, the quantity estimated to be necessary to get accurate sequencing data. In addition, a new 479 primer was ordered, further upstream of the desired mutation on the VDR DNA sequence. This new 479 primer was necessary, as the region of the desired mutation at 143 was too close to the 502 primer.

The double mutant was verified using both the 479 and 824 primers to sequence both the desired mutations in the VDR DNA sequence.

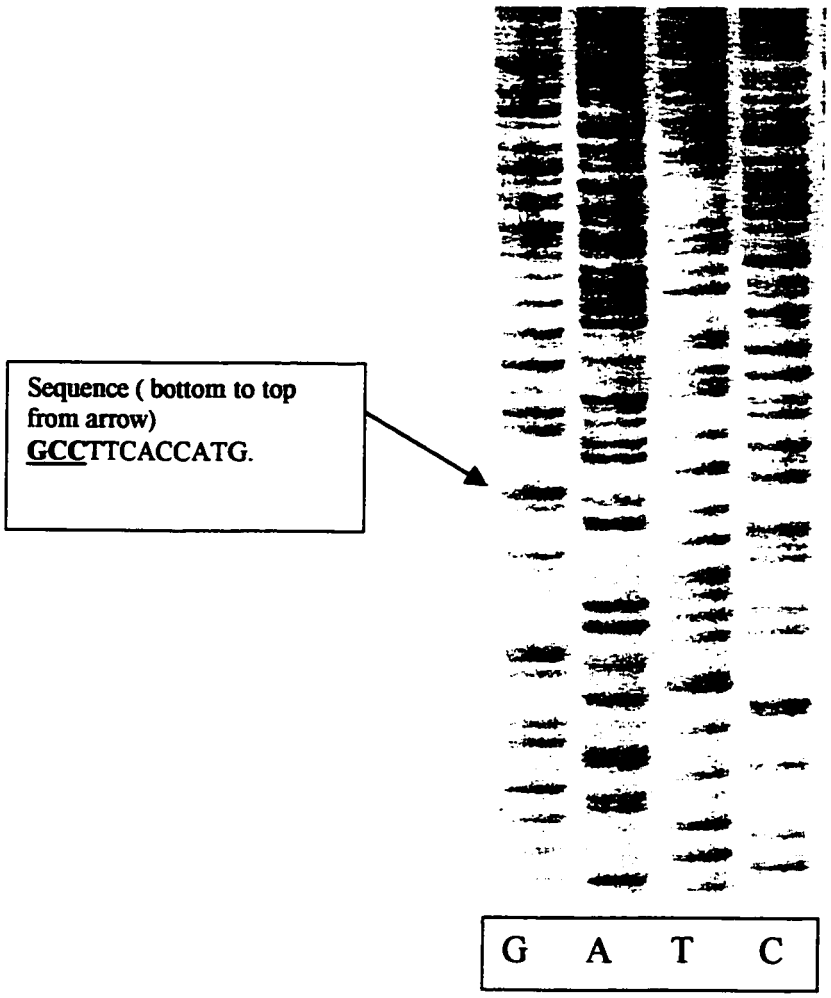

Figure 7- Sequencing Gel Showing GCC Mutation of VDR S278A DNA. Mini plasmid prep of a positive colony for the 278 mutation was sequenced using the 824 primer, using the Novex SureLock gel apparatus.

5.2 Binding Assays

At least three binding assay trials were done for each mutant. Specific binding was determined at each concentration of [^{3}H]-1,25(OH)$_2$ D$_3$ by averaging the three dpm (disintegrations per minute) values obtained from scintillation counting of the "hot" only vials, and then subtracting the average dpm value of the "hot + excess cold" vials. This

results in one specific binding dpm value for each concentration. Two trials had points excluded from the hot tube average, by use of the Q test of Dean and Dixon (Jack, 1995). See appendix D for the exact points excluded. The specific binding dpm value was converted to femtomoles of receptor using the equations:

(Specific binding dpm) / (2.22 x 10^{12} dpm/Ci) = Ci of [^{3}H]-1α,25(OH)$_2$ D$_3$

(Ci of [^{3}H]-1,25(OH)$_2$ D$_3$) * (1.00 x 10^{12} fmol [^{3}H]-1,25(OH)$_2$ D$_3$/168 Ci) = fmol receptor

The value of 2.22 x 10^{12} dpm/Ci is a standard value for the number of disintegrations per minute per Curie, while the 10^{12} fmol [^{3}H]-1,25(OH)$_2$ D$_3$/168 Ci value is the specific activity of the [^{3}H]-1,25(OH)$_2$ D$_3$. The specific activity value was different for each batch of [^{3}H]-1,25(OH)$_2$ D$_3$ used. The specific binding data was entered into GraphPad Prism software, version 3.2, and analyzed using nonlinear regression. The data was fit to the one-site binding equation:

$$Y = \frac{B_{max} * X}{K_d + X}$$

The program generates a calculated K_d and B_{max} value, along with sigma and R^2 value to determine the "goodness of fit" of the data to the equation. K_d values were considered valid if the R^2 value was above 0.90. Data was plotted for each trial using the graphing

routine in the GraphPad Prism software. Error bars for total and non-specific binding are +/-1 sigma values. Specific binding curves are fit to a single point for each concentration of $1,25(OH)_2 D_3$, and so do not have error bars. Figures 8-11 show representative saturation binding graphs for the wild type and each mutant VDR. Figure 12 is a compilation of representative graphs of specific binding for wild type and each mutant VDR. Summary data for all trials is shown in Table 9. Raw data for each trial is shown in Appendix D.

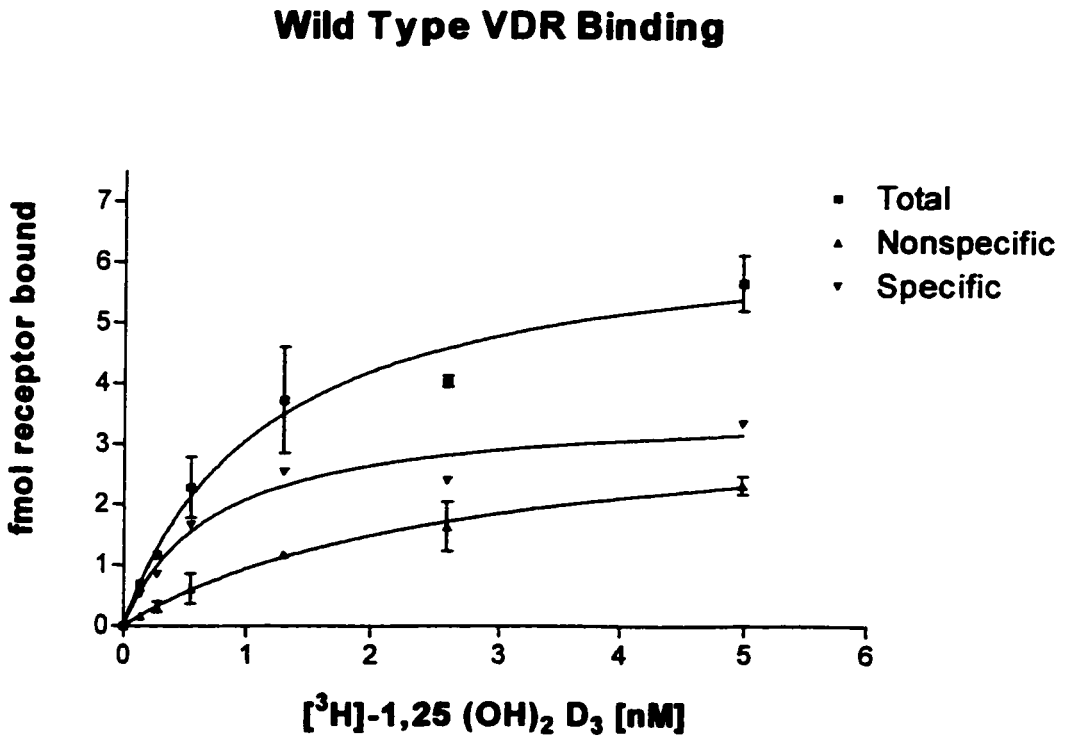

Figure 8- Saturation Analysis of Wild Type Mutant. Cos-1 cells were harvested and homogenized in TED buffer, pH 7.5.. Aliquots of 0.1 mL were incubated for 4 hours on ice with [^{3}H]-1,25(OH)$_2$ D$_3$ (specific activity 168 Ci/mmole) at concentrations varying from 0.125 nM to 5.0 nM, in the presence or absence of 500 nM nonradioactive 1,25(OH)$_2$ D$_3$. Hormone bound to receptor was separated from free ligand using the hydroxylapatite batch assay. Data for total binding are the mean of triplicate points; non-specific data are the mean of duplicate points. Specific binding is calculated by subtracting non-specific binding from total binding. K_d for this trial= 0.721 +/- 0.199 nM, R^2=0.966

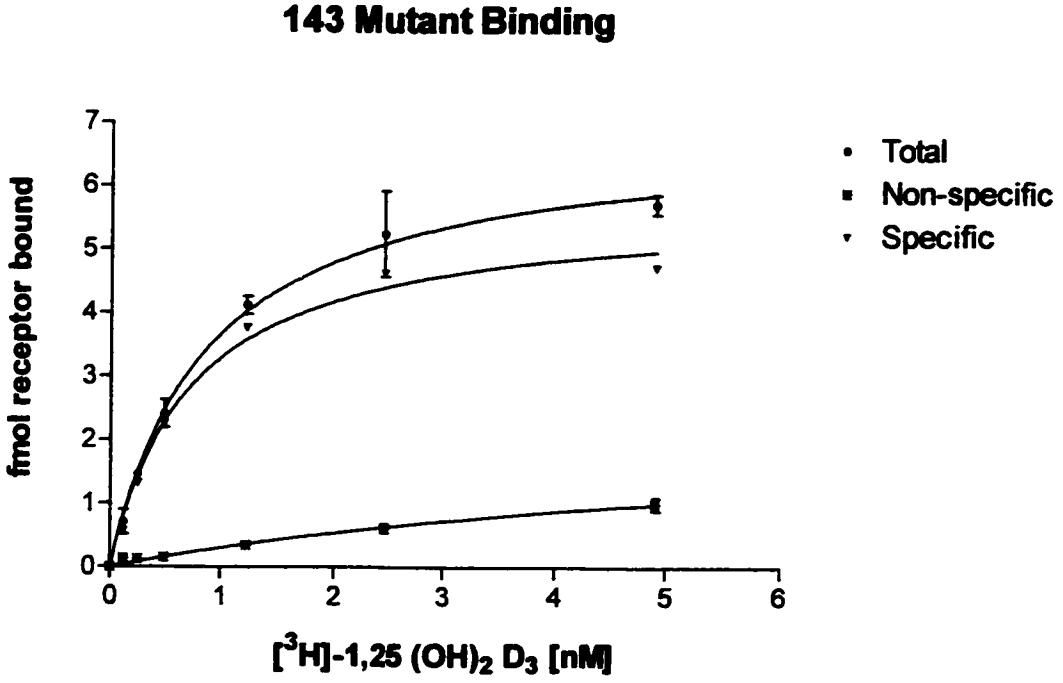

Figure 9- Saturation Analysis of 143 Mutant. Cos-1 cells were harvested and homogenized in TED buffer, pH 7.5. Aliquots of 0.1 mL were incubated for 4 hours on ice with [^{3}H]-1,25(OH)$_2$ D$_3$ (specific activity 168 Ci/mmole) at concentrations varying from 0.125 nM to 5.0 nM, in the presence or absence of 500 nM nonradioactive 1,25(OH)$_2$ D$_3$. Hormone bound to receptor was separated from free ligand using the hydroxylapatite batch assay. Data for total binding are the mean of triplicate points; non-specific data are the mean of duplicate points. Specific binding is calculated by subtracting non-specific binding from total binding. K_d for this trial= 0.828 +/- 0.140 nM., R^2=0.990.

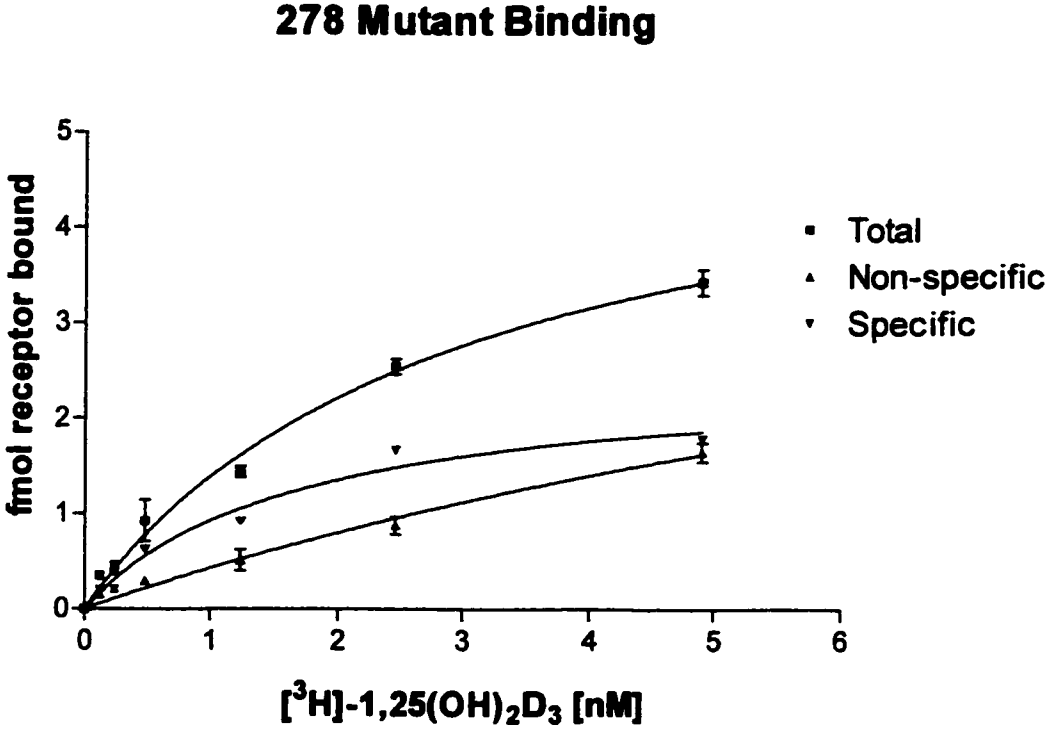

Figure 10-Saturation Analysis of 278 Mutant. Cos-1 cells were harvested and homogenized in TED, pH 7.5. Aliquots of 0.1ml were incubated for 4 hours on ice with [^{3}H]-1,25(OH)$_2$ D$_3$ (specific activity 168 Ci/mmole) at concentrations varying from 0.125 nM to 5.0 nM, in the presence or absence of 500 nM nonradioactive 1,25(OH)$_2$ D$_3$. Hormone bound to receptor was separated from free ligand using the hydroxylapatite batch assay. Data for total binding are the mean of triplicate points; non-specific data are the mean of duplicate points. Specific binding is calculated by subtracting non-specific binding from total binding. K_d for this trial= 1.72 +/- 0.491 nM, R^2=0.976.

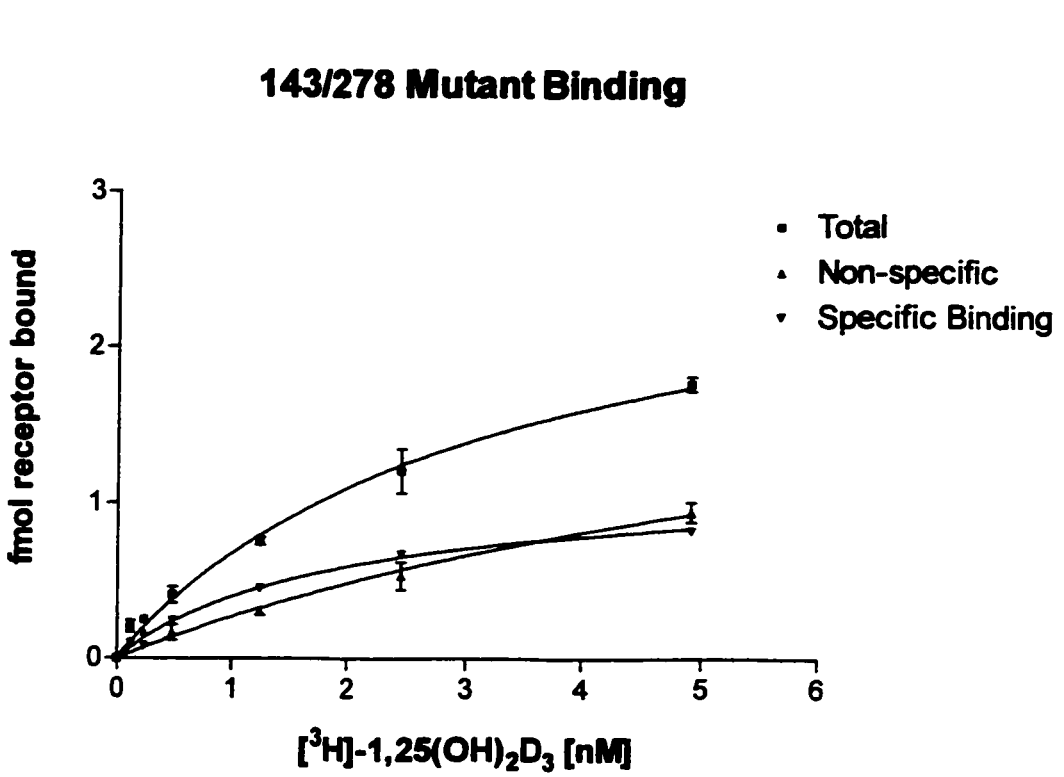

Figure 11-Saturation Analysis of 143/278 Mutant. Cos-1 cells were harvested and homogenized in TED buffer, pH 7.5. Aliquots of 0.1 mL were incubated for 4 hours on ice with [^{3}H]-1,25(OH)$_2$ D$_3$ (specific activity 168 Ci/mmole) at concentrations varying from 0.125 nM to 5.0 nM, in the presence or absence of 500 nM nonradioactive 1,25(OH)$_2$ D$_3$. Hormone bound to receptor was separated from free ligand using the hydroxylapatite batch assay. Data for total binding are the mean of triplicate points; non-specific data are the mean of duplicate points. Specific binding is calculated by subtracting non-specific binding from total binding. K_d for this trial= 1.92 +/- 0.291 nM, R^2=0.994.

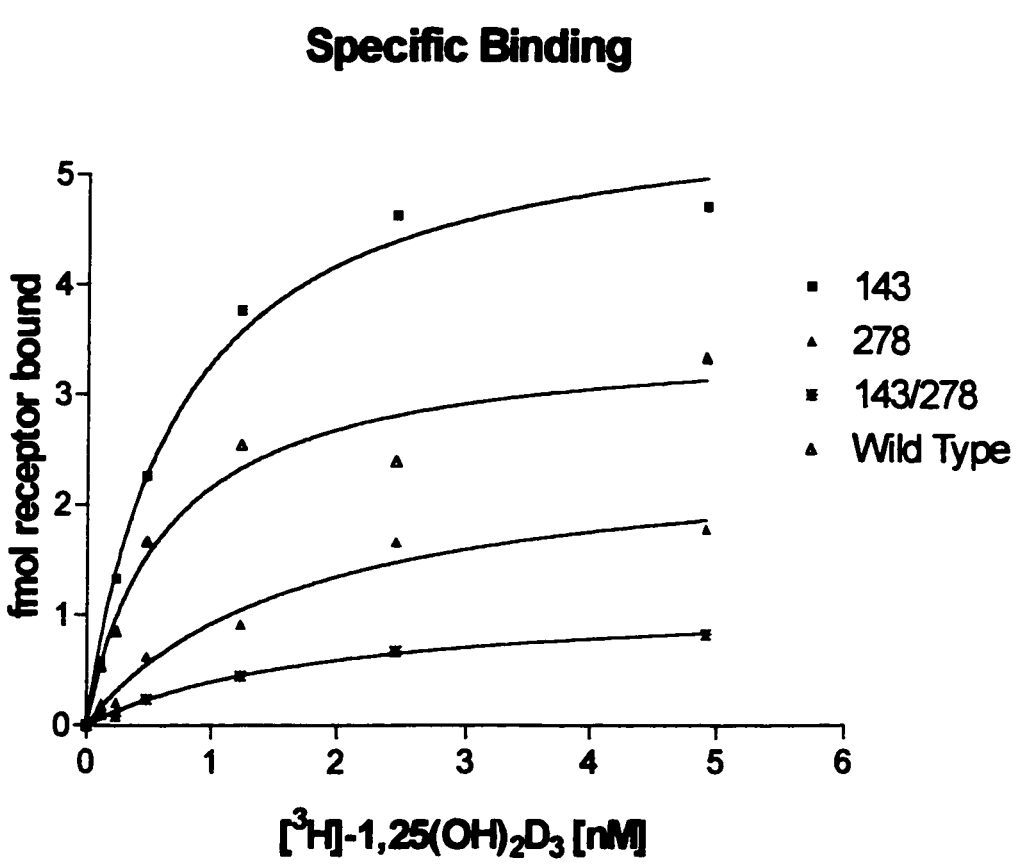

Figure 12- Specific Binding Curves for 143, 278, 143/278, and Wild Type VDR. Cos-1 cells were harvested and homogenized in TED buffer, pH 7.5. Aliquots of 0.1 mL were incubated for 4 hours on ice with [^{3}H]-1,25(OH)$_2$ D$_3$ (specific activity 168 Ci/mmole) at concentrations varying from 0.125 nM to 5.0 nM, in the presence or absence of 500 nM nonradioactive 1,25(OH)$_2$ D$_3$. Hormone bound to receptor was separated from free ligand using the hydroxylapatite batch assay. Data for total binding are the mean of triplicate points; non-specific data are the mean of duplicate points. Specific binding is calculated by subtracting non-specific binding from total binding. K_d for these trials: 143 Mutant= 0.828 +/- 0.130 nM., R^2=0.990, 278 Mutant== 1.72 +/- 0.491 nM, R^2=0.976, 143/278 Mutant= 1.92 +/- 0.291 nM, R^2=0.994, Wild Type VDR= 0.721 +/- 0.199 nM, R^2=0.966.

Table 9- Summary of Binding Assay Data

Mutant	K_d value-nM	K_d sigma	R^2	Date
143	0.480	0.238	0.911	12/18/01
143	1.29	0.140	0.996	1/18/02
143	0.828	0.130	0.990	1/29/02
143	0.987	0.244	0.974	2/4/02
278	0.916	0.255	0.971	1/8/02
278	1.81	0.405	0.985	1/8/02
278	1.72	0.491	0.976	2/4/02
278	0.503	0.134	0.966	3/5/02
143/278	1.92	0.291	0.994	1/18/02
143/278	1.34	0.260	0.987	1/29/02
143/278	0.589	0.186	0.954	3/4/02
Wild Type VDR	0.904	0.307	0.956	11/27/01
Wild Type VDR	0.739	0.323	0.923	3/4/02
Wild Type VDR	0.721	0.199	0.966	3/5/02

5.3 Statistical Analysis of Binding Assay Data

Statistical data for the binding assay trials is summarized in Table 9. Data for the trials was compared to wild type data using the student's unpaired t-test, using criteria of $P < 0.05$ to determine a difference in population means. The t-test data shows no

statistically significant difference between the means of the wild type VDR trials and any of the mutant population means.

Table 10- Statistical Summary Data of Binding Assay Trials

VDR Type	Mean of trials (nM) +/- sigma	N	t value	P value
Wild type	0.788 +/- 0.058	3		
143 mutant	0.896 +/- 0.168	4	0.527	0.621
278 mutant	1.24 +/- 0.316	4	1.19	0.288
143/278 mutant	1.28 +/- 0.383	3	1.27	0.272

6.0 Discussion

The mechanism of how $1,25(OH)_2D_3$ influences biological actions in the human body is extremely complicated and has been the subject of much study. The $1,25(OH)_2D_3$ binds to its nuclear receptor (Haussler & Brumbaugh, 1975), promotes the formation of VDR-retinoid X receptor heterodimers, and this complex binds to vitamin D response elements on target genes (Peleg, Sastry, Collins, Bishop, & Norman, 1995). Expression of these target genes can be either stimulated or repressed as a result of the ligand-receptor interaction.

The exact nature of the ligand-VDR binding has been difficult to determine due to the unusual conformational flexibility of $1,25(OH)_2D_3$ compared to other steroid hormones. The A ring of $1,25(OH)_2D_3$ assumes two chair conformations in solution, and the side chain may assume many different conformations due to single bond rotation. The ability of many different analogs of $1,25(OH)_2D_3$ to bind with similar affinity as the natural ligand indicates that the ligand binding pocket of VDR can accommodate a variety of conformations of $1,25(OH)_2D_3$. However, while many analogs bind with similar affinity as $1,25(OH)_2D_3$, their ability to effect transactivation of target genes may differ significantly from the natural ligand. This indicates conformational differences in the ligand-receptor complex that may be caused by analog interaction with different residues within the ligand binding pocket of VDR.

The ligand binding domain of VDR, and other nuclear receptors in the same superfamily, consists of 12 α-helices and several short β-strands organized around a lipophilic hormone-binding pocket (Petkovich, Brand, Krust, & Chambon, 1987). When

the structure of VDR is compared to other nuclear receptors there is an additional loop region in the protein connecting helices 1 and 3. This loop region varies from 72 to 81 residues in the VDR family. This variation has allowed for several different models of the helix structure of VDR to be developed. Models with a longer loop region are more homologous to retinoic acid receptors, models with a shorter loop region are more homologous to thyroid receptors. The lack of defined secondary structure in this loop and the large size of VDR have made it difficult to crystallize the entire structure for analysis.

The ligand binding domain of VDR was crystallized with a deletion of residues 165-215 (Rochel *et al.*, 2000). The three hydroxyl groups of the ligand are stabilized by hydrogen bonding to polar residues within the hydrophobic pocket of the ligand binding domain. The "straight down" conformation of the truncated loop between helix 1 and helix 3 in the crystal structure of the ligand binding domain of VDR brings residue 143 of VDR into close enough contact with the 3-OH group of the hormone to be a hydrogen bond donor. The other predicted hydrogen bond donor for the 3-OH group, residue 278, is located in helix 5 in the crystal structure. The truncated loop position in the crystal structure resembles the loop position found in the estrogen and progesterone receptors, which belong to a different nuclear receptor subfamily than VDR (Choi *et al.*, 2001).

In this work, site-directed mutagenesis was used to generate three mutant VDRs in order to investigate the residues 143 and 278 identified as hydrogen bond donors for the 3-OH group by the crystal structure data. Residue 143 was mutated from a tyrosine to a phenylalanine, and residue 278 was mutated from a serine to an alanine. A double mutant containing both mutations was also generated. The site-directed mutagenesis was

successful, and all three mutant VDRs were sequenced to verify the presence of only the desired mutation. The wild type and mutant VDR proteins were produced in COS-1 cells transfected with the plasmid containing the appropriate cDNA. Binding assays were performed on cell lysates and K_d values calculated. K_d values for all three mutants were determined from a minimum of three trials and compared to wild type VDR K_d. No statistical difference between the K_d values for Y143F, S278A or Y143F/S278A VDR and wild type VDR was found. This means that mutating residues 143 and 278 from polar residues to non-polar residues did not reduce binding affinity of the ligand to the receptor.

There are several possible explanations for the results obtained in this work. Analog data indicates the 3-OH group is not as critical to ligand binding as the 1-OH or 25-OH group. In a 1995 study, Bouillon, Okamura, and Norman reported relative competitive index (RCI) data for 25-(OH)-D_3, 3-dexoy-1,25$(OH)_2D_3$, and 1-$(OH)_2D_3$. RCI measures the relative ability of an analog under *in vitro* conditions to compete with [^{3}H]-1,25$(OH)_2D_3$ for binding to VDR (see section 2.1 for a description of RCI calculation). An RCI value of 0.25 for an analog represents a binding affinity for the analog equal to 0.25% of the natural ligand binding affinity. The RCI value for 25-(OH)-D_3 was reported as 0.15, the 1-$(OH)_2D_3$ value reported as 0.17, but 3-deoxy-1,25$(OH)_2D_3$ was reported as 3-13 (4 different studies). This data indicates that the 3-OH hydroxyl group is important for ligand binding, but not as important as the 1-OH or 25-OH group. Mutating residues 143 and 278 may not reduce binding affinity if

the hydrogen bonding of the 3-OH group is not critical to the overall binding affinity of the ligand to the receptor.

Another possible explanation for the experimental results is that other surrounding residues could be forming alternate hydrogen bonds with the 3-OH group when the polar residues 143 and 278 are mutated. There are several other possible residues within the ligand binding pocket that could be in proximity to form alternate bonds. Other possible residues located near residue 143 are 148-tyrosine and 149-serine. Possible alternate residues located near residue 278 are 275-serine and 274-arginine.

A third possible explanation for the experimental results is the crystal structure may have a different conformation than the wild type receptor due to the deletion of residues 165-215. The two models and the crystal structure differ significantly in their prediction of the hydrogen bond residues for the 3-OH group, due to different assignments of residues to helices 1, 2, 3, and the loop region. In particular, the location of residue 143 is very different. The Yamamoto *et al.* (1999) model leaves this residue out of the ligand binding domain entirely, citing that it is not conserved in all species. Residue 143 is a nonpolar phenylalanine residue in chick and frog VDR (Acevedo & Collins, 2002), so the assumption of the Yamamoto *et al.* model may be correct. The Norman *et al.* (1999) model excludes residue 143 from the helices, and places it outside the ligand binding pocket. The experimental data for the 143 mutant in this study indicates that the binding affinity is not reduced and therefore the tyrosine at residue 143 does not appear to be important for ligand binding. This work suggests that residue 143 may not be in ligand binding pocket of the receptor.

The experimental data obtained in this work for S278A also suggests that this residue may not be forming a hydrogen bond. Additional binding data published by Yamamoto *et al.* in 2000 showed binding affinity of S278A to be just slightly lower than wild type VDR, although no K_d value was reported. The crystal structure identification of residue 278 again suggests that the deletion of residues 165-215 may result in a receptor with an alternate conformation in this region. While the Yamamoto *et al* and Norman *et al.* models place residues 275, 278, and 288 in slightly different positions in the receptors, the binding data of mutants indicates that residues 275 and 288 are likely candidates for interaction with the 3-OH group.

Residue C288 is predicted to be a hydrogen bond donor for the 3-OH group by the Yamamoto *et al.* model, and mutational studies done by the same group show reduced binding affinity when C288 is replaced by alanine. If the A-ring of $1,25(OH)_2 D_3$ were to adopt an A conformation instead of the B conformation in the crystal structure, then the 3-OH group is close enough to residue 288 to form a hydrogen bond (Choi *et al.*, 2001). The Yamamoto group assigned cysteine 288 as the most likely hydrogen bond donor for the 3-OH group, based on the significant reduction in binding affinity when this residue is mutated to alanine. As this residue is conserved in human, rat, mouse, and avian VDR, (Nakajima *et al.*, 1996) it seems likely to be have an important structural or functional role in the receptor.

The experimental results obtained for the binding affinity of the three mutants, Y143F, S278A, and Y143F/S278A indicates that neither residue had a measurable affect on binding affinity of $1,25(OH)_2 D_3$. This experimental data suggests that the deletion of

residues 165-215 may change the conformation of the N-terminal region of the wild-type VDR ligand binding domain helices 1-3. Although the 3-OH group of the hormone is not as important for binding as the 1- or 25-OH groups, lack of the 3-OH group reduces ligand binding by 90%. If residues 143 and 278 form hydrogen bonds with the 3-OH group then loss of those hydrogen bonds should also decrease binding affinity. Since mutation of either residue or both residues had no effect on binding affinity it seems unlikely that these residues actually form hydrogen bonds with the hormone or else those hydrogen bonds do not contribute much to the overall binding. One of the models of the ligand binding domain may more accurately represent the residues in contact with the 3-OH group.

Further experiments will need to be performed to define the role of residues 143 and 278 in the ligand binding domain. One possible experiment is to generate mutations of both these residues using a VDR ligand binding domain with the same residues deleted as in the crystal structure. Using this deletion mutant would allow for the same VDR ligand binding domain conformation that is evident in the crystal structure. If the 143 and 278 mutants within the deletion mutant ligand binding domain show reduced binding affinity compared to the wild type deletion mutant then this would suggest that the crystal structure is not identical to the full-length wild type receptor.

The crystal structure of the ligand binding domain of VDR and two models examined in this study have reasonable agreement on the residues within VDR that form hydrogen bonds with the 1 and 25-OH groups of the ligand $1,25(OH)_2D_3$. This work indicates that

there is still uncertainty regarding the residues forming hydrogen bonds with the 3-OH group of $1,25(OH)_2D_3$.

7.0 Conclusion

Three mutants of human vitamin D nuclear receptor were produced using site-directed mutagenesis. Residues were chosen based on X-ray crystallography data of the ligand binding domain of vitamin D nuclear receptor, which showed residues 143 and 278 making hydrogen bonds with the 3-OH group of the ligand $1,25(OH)_2D_3$. Residue 143 was mutated from tyrosine to phenylalanine, residue 278 was mutated from serine to alanine, and a double mutant with both mutations was created. The mutated cDNA was sequenced for all three mutants to verify the presence of only the desired mutation. The mutated cDNA was then used to generate the vitamin D nuclear receptor protein with the desired residue change. Binding assays were then performed to determine if the residue change resulted in any change in binding affinity of $1,25(OH)_2D_3$ to the receptor. For both single mutants and the double mutant, no statistically significant change in binding affinity compared to wild type receptor was found. These results were not expected, and there are several possible explanations for the results obtained. The 3-OH group may not be critical for ligand binding, other residues may be able to form compensating hydrogen bonds, or the VDR ligand binding domain with residues 165-216 deleted may be assuming an unnatural conformation in the crystal structure. Further work is necessary to distinguish between these possibilities.

8.0 References

Acevedo, A., Collins, E. (2002) [VDR cDNA sequence comparison between species]. Unpublished data.

Askew, R. A., Bourdillon, R. B., Burce, H. M., Jenkins R. G. C., Webster, T. A. (1931). The distillation of vitamin D. Proceedings of the Royal Society (London) Biological Sciences, 107, 76-90.

Baker, A. R., McDonnel, D. P., Hughes, M., Crisp T. M., Mangelsdorf, D. J., Haussler, M. R., Pike, J. W., Shine J., O'Malley B. W. (1988). Cloning and expression of full-length cDNA encoding human vitamin D receptor. Proceedings of the National Academies of Sciences U.S.A., 85, 3294-3298.

Binderup, L., Latini, S., Binderup, E., Bretting, C., Calverley, M., Hansen, K. (1991). 20-epi-vitamin D3 analogues: a novel class of potent regulators of cell growth and immune responses. Biochemical Pharmacology, 42,1565-1575.

Binderup, L. (1993). Comparison of cacipotriol with selected metabolites and analogues of vitamin D3: effects on cell growth regulation *in vitro* and calcium metabolism *in vivo*. Pharmacology & Toxicology, 72, 240-244.

Blunt, J. W., DeLuca, H. F., Schones, H. K. (1968). 25-hydroxycholecalciferol. A biologically active metabolite of vitamin D3. Biochemistry, 7, 3317-3322.

Bouillon, R., Okamura, W. H., Norman, A. W. (1995). Structure-function relationships in the vitamin D endocrine system. Endocrinology Reviews, 16, 200-257.

Bourguet, W., Ruff, M., Chambon, P., Gronemeyer, H., Moras, D. (1995). Crystal structure of the ligand-binding domain of the human nuclear receptor RXR-alpha. Nature 375, 377-382.

Burmester, J. K., Wiese, R. J., Maeda, N., DeLuca, H. F. (1988). Structure and regulation of the rat 1,25-dihydroxyvitamin D3 receptor. Proceedings of the National Academy of Sciences U.S.A., 85, 9499-9502.

Cheskis, B., Freedman L.P. (1994) Ligand modulates the conversion of DNA-bound vitamin D3 receptor (VDR) homodimers into VDR-retinoid X receptor heterodimers. Molecular and Cellular Biology, 14, 3329-3338.

Choi, M., Yamamoto, K., Masuno, H., Nakashima, K., Taga, T., Yamada, S. (2001). Ligand recognition by the vitamin D receptor. Bioorganic & Medicinal Chemistry, 9, 1721-1730.

Collins, E.D., Norman, A.W. (2000). Studies identifying key interaction points between 1,25-dihydroxyvitamin D_3 and the ligand binding domain of the vitamin D nuclear receptor using molecular modeling and site-directed mutagenesis. In Norman, A. W., Bouillon, R., Thomasset, M. (Ed.). Vitamin D Endocrine System Structural, Biological, Genetic, and Clinical Aspects (pp. 251-258). University of California Riverside Printing and Reprographics.

Collins, E. D., Norman, A. W. (2001). Vitamin D. In R. Rucker, J. Suttie, D. McCormick and L. Machlin (Ed.) Handbook of Vitamins (pp. 51-113). New York: Marcek Dekker, Inc.

Collins, E. D. (1994). Structure/function and molecular studies of the chick intestinal and HL-60 cell nuclear 1α, 25-dihydroxyvitamin D_3 receptor; production of monospecific polyclonal antibodies to the human 1α,25-dihydroxyvitamin-D_3 receptor; and molecular cloning of a new member of the steroid/vitamin D/thyroid superfamily of nuclear hormone receptors. Unpublished Ph.D. Dissertation, University of California, Riverside, CA.

Colnot, S., Lambert, M., Blin, C., Thomasset, M., Perret, C. (1995). Identification of DNA sequences that bind retinoid X receptor-1,25$(OH)_2$ D_3- receptor heterodimers with high affinity. Molecular Cell Endocrinology, 113, 89-98.

Conlan, R., & Sherman, E. Unraveling the enigma of vitamin D. The National Academies. <http://www4.nationalacademies.org/beyond/beyonddiscovery> (2001, February 15).

DeLuca, H. F. (1995). Discovery of the vitamin D endocrine system. Experimental Biology 95.

Feng, W., Ribeiro, R. C. J., Wagner, R. L., Nguyen, H., Apriletti, J.W, Fletterick, R.J., Baxter, J.D., Kusher, P.J., West, B.L. (1998). Hormone-dependent coactivator binding to a hydrophobic cleft on nuclear receptors. Science, 280, 1747-1749.

Fraser, D. R., Kodicek, E. (1970). Unique biosynthesis by kidney of a biological active vitamin D metabolite. Nature, 228, 764-766.

Gray, R., Boyle, I., DeLuca, H. F. (1971). Vitamin D metabolism: the role of kidney tissue. Science, 172, 1232-1234.

Haussler, M. R., Whitfield, G. K., Haussler, C. A., Hsieh, J-C., Thompson, P. D., Selznick, S. H., Dominguez, C. E., Jurutka, P. W. (1998). The nuclear vitamin D receptor: biological and molecular properties revealed. Journal of Bone and Mineral Research, 13, 325-349.

Haussler, M. R., Brumbaugh, P. F. (1975). Specific binding of 1alpha,25-dihydroxycholecalciferol to nuclear components of chick intestine. Journal of Biological Chemistry, 250, 1588-94.

Haussler, M. R., Haussler, C. A., Jurutka, P. W., Hsieh, J., Remus, L. S., Selznick, S. H., Whitfield, G. K. (1997). The vitamin D hormone and its nuclear receptor: molecular actions and disease states. Journal of Endocrinology, 154, S57-S73.

Henry, H. L., Dutta, C., Cunningham, N., Blanchard, R., Penny, R., Tang, C., Marchetto, G., Chow, S-Y. (1992). The cellular and molecular regulation of 1,25 $(OH)_2D_3$ production. The Journal of Steroid Biochemistry and Molecular Biology, 41, 401-407.

Herdick, M., Bury, Y., Quack, M., Uskokovic, M. R., Polly, P. (2000). Response element and coactivator-mediated conformational change of the vitamin D_3 receptor permits sensitive interaction with agonists. Molecular Pharmacology, 57, 1206-1217.

Iida, K., Shinki, T., Yamaguchi, A., DeLuca, H. F., Kurokawa, K., Suda, T. (1995). A possible role of vitamin D receptors in regulating vitamin D activation in the kidney. Proceedings of the National Academy of Sciences U.S.A, 92, 6112-6116.

Jack, R. (1995). Basic Biochemical Laboratory Procedures and Computing. (pp. 330). New York: Oxford University Press.

Jiménez-Lara, A. M., & Aranda, A. (1999). Lysine 246 of the Vitamin D receptor is crucial for ligand-dependent interaction with coactivators and transcriptional activity. The Journal of Biological Chemistry, 274, 13503-13510.

Jin, C. H., Pike, J. W. (1996). Human vitamin D receptor-dependent transactivation in *Saccharomyces cerevisiae* requires retinoid X receptor. Molecular Endocrinology, 10, 196-205.

Jururtka, P. W., Hsieh, J., Remus, L. S., Whitfield, G. K., Thompson, P. D., Haussler, C. A., Blanco, J. C. G., Ozato, K., Haussler, M. R. (1997). Mutations in the 1,25-dihydroxyvitamin D_3 receptor identifying C-terminal amino acids required for transcriptional activation that are functionally dissociated from hormone binding, heterodimeric DNA binding, and interaction with basal transcription factor IIB, *in vitro*. The Journal of Biological Chemistry, 272, 14592-14598.

Kato, S. (2000). The function of vitamin D receptor in vitamin D action. Journal of Biochemistry, 127, 717-722.

Kodicek, E. (1956). Ciba Foundations Symposium on Bone Structure and Metabolism. Wolstrenhome, G .W. E. & O' Connor, C. M. (Ed). (pp. 161-174). Boston: Little, Brown, and Co.

Koszewski, N. J., Reinhardt, T.A., Horst, R. L. (1999). Differential effects of 20-epi vitamin D analogs on the vitamin D receptor homodimer. Journal of Bone and Mineral Research, 14, 509-517.

Kraichely, D. M., Collins III, J. J., DeLisle, R. K., MacDonald, P. N. (1999). The autonomous transcription domain in helix H3 of the vitamin D receptor is required for

transactivation and coactivator interaction. The Journal of Biological Chemistry, 272, 14352-14358.

Kristjansson, K., Rut, A. R., Hewison, M., O'Riordan, J. L. H., Hughes, M. R. (1993). Two mutations in the hormone binding domain of the vitamin D receptor cause tissue resistance to 1,25-dihydroxyvitamin D_3. Journal of Clinical Investigation, 92, 12-16.

Lemire, J. M., Archer, C. D., Khulkarini, A., Ince, A., Uskokovic, M. R., Stephkowski, S. (1992). The vitamin D_3 analogue 1,25 dihydroxy–cholecalciferol prolongs the survival of murine cardiac allografts. Transplantation, 54, 762-763.

Liao, J., Ozono, K., Sone, T., McDonnell, D. P., Pike, J. W. (1990). Vitamin D receptor interaction with specific DNA requires a nuclear protein and 1,25-dihydroxyvitamin D_3. Proceedings of the National Academy of Sciences U.S.A., 87, 9751-9755.

Liberman, U. A. (1996), Hereditary deficiencies in vitamin D action. In Blilezikian, J.P., Raisz, L.G., Rodan, G.A. (Ed). Principles of Bone Biology: (pp. 903-933). San Diego, CA: Academic Press.

Lund, J., DeLuca, H. F. (1966). Biologically active metabolite of vitamin D3 from bone, liver, and blood serum. Journal of Lipid Research, 7, 739-744.

Lui, Y-Y., Collins, E. D., Norman, A. W., Peleg, S. (1997). Differential interaction of 1α,25-dihydroxyvitamin D_3 analogues and their 20-*epi* homologues with the vitamin D receptor. The Journal of Biological Chemistry, 272, 3336-3345.

Lui, Y-Y., Nguyen, C., Peleg, S. (2000). Regulation of ligand-induced heterodimerization and coactivator interaction by the activation function-2 domain of the vitamin D receptor. Molecular Endocrinology, 14, 1776-1787.

MacDonald, P. N., Dowd, D. R., Nakajima, S., Galligan, M. A., Reeder, M. C., Haussler C. A., Ozatao, K., Haussler, M. R. (1993). Retinoid X receptors stimulate and 9-cis retinoic acid inhibits 1,25-dihydroxyvitamin D_3-activated expression of the rat osteocalcin gene. Molecular and Cellular Biology, 13, 5907-5917.

Malloy, P., Eccleschall, T., Gross, C., Van Maldergem, L., Bouillon, R., Feldman, D. (1997). Hereditary vitamin D resistant rickets caused by a novel mutation in the
in D receptor that results in a decreased affinity for hormone and cellular
sponsiveness. Journal of Clinical Investigation, 99, 297-304.

Makin, G., Lohnes, D., Byford, V., Ray, R., Jones, G. (1989). Target cell metabolism for 1,25-dihydroxyvitamin D_3 to calcitroic acid. Evidence for a pathway in kidney and bone involving 24-oxidation. Biochemical Journal, 184, 173-180.

McCutchan, J. H., Pagano, J. S. (1968). Enhancement of the infectivity of simian virus 40 deoxyribonucleic acid with diethylaminoethyl-dextran. Journal of the National Cancer Institute, 41, 351-357.

McCollum, E. V., Simmonds, N., Becker, E., Shipley, P. G. (1922). An experimental demonstration of a vitamin which promotes calcium deposition. Journal of Biological Chemistry, 53, 293-312.

McDonnell, D. P., Scott, R., Kerner, S. A., O'Malley, B. W., Pike, J. W. (1989). Functional domains of the human vitamin D3 receptor regulate osteocalcin gene expression. Molecular Endocrinology, 3, 635-644.

Motulsky, H. (1999). Analyzing radioligand binding data. Analyzing Data with GraphPad Prism. (pp 243-247). GraphPad Software. San Diego, CA.

Nakajima, S., Hsieh, J., Jurutka, P. W., Galligan, M. A., Haussler, C., Whitfield, G. K., Haussler, M. R. (1996). Examination of the potential functional role of conserved cysteine residues in the hormone binding domain of the human 1,25-dihyroxyvitamin D_3 receptor. The Journal of Biological Chemistry, 271, 5143-5149.

Nakajima, S., Yamagata, M., Sakai, N., Ozono, K. (1998). Characterization of the activation function-2 domain of the human 1,25-dihydroxyvitamin D3 receptor. Molecular and Cellular Endocrinology, 136, 15-24.

Nicolaysen, R., Eeg-Larsen, N. (1953). The biochemistry and physiology of vitamin D. Vitamins Hormones, 11, 29-60.

Nishikawa, J., Kitaura, M., Matsumoto, M., Imagawa, M., Nishihara, T. (1994). Difference and similarity of DNA sequence recognized by VDR homodimer and VDR/RXR hetereodimer. Nucleic Acids Research, 22, 2902-2907.

Norman, A. W., Lund, J., DeLuca, H. F. (1964). Studies on calciferol metabolism. I. Production of vitamin D metabolite 4B from 25-OH-cholecalciferol by kidney homogenates. Archives of Biochemistry and Biophysics, 120, 293-312.

Norman, A. W., Midgett, R. J., Myrtle, J. F., Nowick, H. G. (1971). Studies on calciferol metabolism. I. Production of vitamin D metabolite 4B from 25-OH-

cholecalciferol by kidney homogenates. Biochemistry and Biophysics Research Communications, 42, 1082-1087.

Norman, A., Okamura, W., Hammond, M., Bishop, M., Dormanen, M., Rosenfeld, M., Willson, T., Glass, C., Millburn, M. (1997). Comparison of 6-s-*cis*- and 6-s-*trans*-locked analogs of 1a,25-dihydroxyvitamin D3 indicates that the 6-s-*cis* conformation is preferred for rapid nongenomic biological responses and that neither 6-s-*cis* nor 6-s-*trans* locked analogs are preferred for genomic biological responses. Molecular Endocrinology 11, 1518-1531.

Norman, A. W., Adams, D., Collins, E. D., Okamura, W. H., Fletterick, R. J. (1999). Three-dimensional model of the ligand binding domain of the nuclear receptor for 1α,25-dihydroxy-vitamin D_3. Journal of Cellular Biochemistry, 74, 323-333.

Okamura, W. H., Norman, A. W., Wing, R. M. (1974). Vitamin D: concerning the relationship between molecular topology and biological function. Proceedings of the National Academy of Sciences U.S.A., 71, 4194-4197.

Okamura, W.H., Do, S.,Kim, H.,Tan, E., Tham, F.,Jeganathan, S., Ferrero, M., Norman, A. W. (2000). Constitutional and conformational isomers of 1α,25-dihydroxyvtiamin D_3 and its metabolites. In Norman, A. W., Bouillon, R., Thomasset, M. (Ed.). Vitamin D Endocrine System. Structural, Biological, Genetic and Clinical Aspects. (pp: 11-22). University Of California Riverside Printing and Reprographics.

O'Riordan, J. L. H. (1997). Rickets, from history to molecular biology, from monkeys to YACS. Journal of Endocrinology, 154, S3-S13.

Owen, I. (1889). Geographical distribution of rickets, acute and sub-acute rheumatism, chorea, cancer and urinary calculus in the British Islands. British Medical Journal, I, 113-116.

Palm, T.A. (1890). The geographical distribution and aetiology of rickets. Practioner, 45, 270-279.

Peleg, S., Sastry, M., Collins, E. D., Bishop, J. E., Norman, A. W. (1995). Distinct conformational changes induced by 20-epi analogues of 1a,25-dihydroxyvitamin D_3 are associated with enhanced activation of the vitamin D receptor. Journal of Biological Chemistry, 270, 10551-10558.

Petkovich, M., Brand, N. J., Krus, T. A., Chambon, P. (1987). A human retinoic receptor which belongs to the family of nuclear receptors. Nature, 330, 444-450.

Rachez, C,. Freedman, L. P. (2000). Mechanisms of gene regulation by vitamin D_3 receptor: a network of coactivator interactions. Gene, 246, 9-21.

Ritchie, H. H., Hughes, M. R., Thompson, E. T., Malley, P. J., Hockberg, Z., Feldman, D., Pike, J. W., O'Malley, B. W. (1989). An ochre mutation in the vitamin D receptor gene causes hereditary 1,25-dihydroxy-vitamin D3 resistant rickets in three families. Proceedings of the National Academy of Sciences U.S.A., 86, 9783-9787.

Rochel, N., Wurtz, J. M., Mitschler, A., Klaholz, B., Moras, D. (2000). The crystal structure of the nuclear receptor for vitamin D bound to its natural ligand. Molecular Cell, 5, 173-179.

Sasaki, H., Harada, H., Handa, Y., Morino, H., Suzawa, M., Shimpo, E., Katsumata, T., Mashuiro, Y., Matsuda, K., Ebihara, K., Ono, T., Masushige, S., Kato, S.

(1995). Transcriptional activity of a fluorinated vitamin D analog on VDR-RXR-mediated gene expression. Biochemistry, 34, 370-377.

Selden, R. F., Howie, K. B., Rowe, M. E., Goodman, H. M., Moore, D. D. (1986). Human growth hormone as a reporter gene in regulation studies employing transient gene expression. Molecular and Cellular Biology, 6 , 3173-3179.

Siebert, P., Ohnuma, N., Norman, A. W. (1979). Studies on the mode of action of calciferol. XXII. A 24*R*-hydroxyl group can replace the 25-hydroxyl group of 1α,25-dihydroxyvitamin D_3 intestinal receptors. Biochemical Biophysical Research Communications 91, 827.

Solomon, C., Macoritto, M., Gao, X-L., White, J. H., Kremer, R. (2001). The unique tryptophan residue of the vitamin D receptor is critical for ligand binding and transcriptional activation. Journal of Bone and Mineral Research, 16, 39-45.

Steenbock, H. (1924). The induction of growth promoting and calcifying properties in a ration by exposure to light. Science, 60, 224-225.

Takeyama, K-I., Yoshikazu, M., Fuse, H., Endoh, H., Murayama, A., Sachiko, K., Suzawa, M., Yanagisawa, J., Kato, S. (1999). Selective interaction of vitamin D receptor with transcriptional coactivators by a vitamin D analog. Molecular and Cellular Biology, 19, 1049-1055.

Taymans, S., Pack, S., Pak, E. (1999).The human vitamin D receptor gene (VDR) is localized to region 12cen-q12 by fluorescent in situ hybridization and radiation hybrid mapping: genetic and physical VDR map. Journal of Bone and Mineral Research, 14, 1163-6.

Thompson, E., Kristjansson, K., Hughes, M. R. (1991). Molecular scanning methods for mutation detection: application to the 1,25-dihydroxyvitamin D receptor. Eighth Workshop on Vitamin D: Abstract Book 6.

Väisänen, S., Juntunen, K., Itkonen, A., Vihko, P., Mäenpää, P. (1997). Conformational studies of human vitamin-D receptor by antipeptide antibodies, partial proteolytic digestion and ligand binding. European Journal of Biochemistry, 248, 156-162.

Väisänen, S., Rouvinen, J., Mäenpää, P. H. (1998). Putative helices 3 and 5 of the human vitamin D_3 receptor are important for the binding of calcitriol. FEBS Letters, 440, 203-207.

Voet, D., & Voet, J. Biochemistry, Second Edition, 1275-1276, New York, John Wiley & Sons, Inc.

Whitfield, G. K., Hsieh, J. C., Nakajima, S., MacDonald, P. N., Thompson, P. D., Jurutka, P. W., Thompson, P. D., Lee, S. M., Zerwekh, J. E., Haussler, M. R. (1995). A highly conserved region in the hormone-binding domain of the human vitamin D receptor contains residues vital for heterodimerization with retinoid X receptor and for transcriptional activation. Molecular Endocrinology, 9, 1166-1179.

Whitfield, G. K., Selznick, S. H., Haussler, C. A., Hsieh, J. C., Galligan, M. A., Jurutka, P. W., Thompson, P. D., Lee, S. M., Zerwekh, J. E., Haussler, M. R. (1996). Vitamin D receptors from patients with resistance to 1,25-dihydroxyvitamin D_3: point mutations confer reduced transactivation in response to ligand and impaired interaction

with the retinoid X receptor heterodimer partner. Molecular Endocrinology, 10, 1617-1631.

Windhaus, A., Schenck, F., von Werder, F. (1936) Uber das antirachitisch wirksame bestranlungsprodukt aus 7-dehydrocholesterin. Hoppe-Seyler's Zeitshcrift für Physiologishe Chemie., 241, 100-103.

Yamamoto, K., Masuno, H., Choi, M., Nakashima, K., Taga, T., Ooizumi, H., Umesono, K., Sicinska, W., VanHooke, J., DeLuca, H., Yamada, S. (1999). Three-dimensional modeling of and ligand docking to vitamin D receptor ligand binding domain. Proceedings of the National Academy of Sciences, 97, 1467-1472.

Appendix A

VDR Amino Acid Sequence and One Letter Amino Acid Abbreviations

A1. Vitamin D Nuclear Receptor Amino Acid Sequence (Baker *et al.*, 1988)

```
  1- MEAMAASTSLPDPGDFDRNVPRICGVCGDRATGFHFNAMT-40

 41- CEGCKGFFRRSMKRKALFTCPFNGDCRITKDNRRHCQACR-80

 81- LKRCVDIGMMKEFILTDEEVQRKREMILKRKEEEALKDSL-120

121-RPKLSEEQQRIIAILLDAHHKTYDPTYSDFCQFRPPVRVN-160

161-DGGGSHPSRPNSRHTPSFSGDSSSSCSDHCITSSDMMDSS-200

201-SFSNLDLSEEDSDDPSVTLELSQLSMLPHLADLVSYSIQK-240

241-VIGFAKMIPGFRDLTSEDQIVLLKSSAIEVIMLRSNESFT-280

281-MDDMSWTCGNQDYKYRVSDVTKAGHSLELIEPLIKFQVGL-320

321-KKLNLHEEEHVLLMAICIVSPDRPGVQDAALIEAOQDRLS-360

361-NTLQTYIRCRHPPPGSHLLYAKMIQKLADLRSLNEEHSKQ-400

401-YRCLSFQPECSMKLTPLVLEVFGNEIS-427
```

A2. Single Letter Abbreviations for Amino Acids

A	Alanine	M	Methionine
B	Asparagine or aspartic acid	N	Asparagine
C	Cysteine	P	Proline
D	Aspartic acid	Q	Glutamine
E	Glutamic acid	R	Arginine
F	Phenylalanine	S	Serine
G	Glycine	T	Threonine
H	Histidine	V	Valine
I	Isoleucine	W	Tryptophan
K	Lysine	Y	Tyrosine
L	Leucine	Z	Glutamine or glutamic acid

Appendix B- pcDNA 1.1/Amp Map

Invitrogen pcDNA 1.1/Amp- 4767 nucleotides
Col E1 origin: bases 1-587
M13 origin: bases 588-1180
Ampicillin gene: bases 1377-2235
T7 primer sequence: bases 2938-2957
Polylinker: bases 2964-3063
Splice and PolyA: bases 3060-3758
Polyomoa origin: bases 3764-4659
SV 40 origin: bases 4600-4767

Eco R1 site: base 3014 G!AATTC
Nsi I site: base 3058 ATGCA ! T

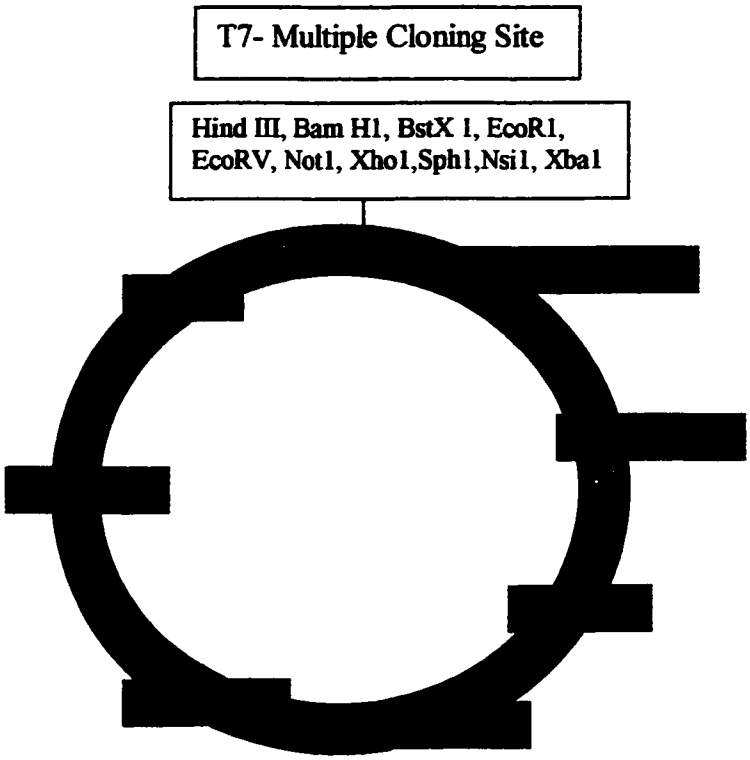

Appendix C-Sequencing Data of Entire VDR Gene for Mutants

143 Mutant- Nucleotide Sequence.
Nucleotide sequence numbering corresponds to nucleotide sequence # J03258 (National Center for Biological Information, May 2002). Codon change is in **bold.**

125 ATGGCGGCCAGCACTTCCCTGCCTGACCCTGGAGACTTTGACCGGA 170
171 ACGTGCCCCGGATCTGTGGGGTGTGTGGAGACCGAGCCACTGGCTTTCA 219
220 CTTCAATGCTATGACCTGTGAAGGCTGCAAAGGCTTCTTCAGGCGAAGC 268
269 ATGAAGCGGAAGGCACTATTCACCTGCCCCTTCAACGGGGACTGCCGCA 317
318 TCACCAAGGACAACCGACGCCACTGCCAGGCCTGCCGGCTCAAACGCTG 366
367 TGTGGACATCGGCATGATGAAGGAGTTCATTCTGACAGATGAGGAAGTG 415
416 CAGAGGAAGCGGGAGATGATCCTGAAGCGGAAGGAGGAGGAGGCCTTGA 464
465 AGGACAGTCTGCGGCCCAAGCTGTCTGAGGAGCAGCAGCGCATCATTGC 513
514 CATACTGCTGGACGCCCACCATAAGACC**TTC**GACCCCACCTACTCCGAC 562
563 TTCTGCCAGTTCCGGCCTCCAGTTCGTGTGAATGATGGTGGAGGGAGCC 611
612 ATCCTTCCAGGCCCAACTCCAGACACACTCCCAGCTTCTCTGGGGACTC 660
661 CTCCTCCTCCTGCTCAGATCACTGTATCACCTCTTCAGACATTGATGGA 709
710 CTCGTCCAGCTTCTCCAATCTGGATCTGAGTGAAGAAGATTCAGATGAC 758
759 CCTTCTGTGACCCTAGAGCTGTCCCAGCTCTCCATGCTGCCCCACCTGG 807
808 CTGACCTGGTCAGTTACAGCATCCAAAAGGTCATTGGCTTTGCTAAGAT 856
857 ATACCAGGATTCAGAGACCTCACCTCTGAGGACCAGATCGTACTGCTGA 905
906 AGTCAAGTGCCATTGAGGTCATCATGTTGCGCTCCAATGAGTCCTTCAC 954
955 CATGGACGACATGTCCTGGACCTGTGGCAACCAAGACTACAAGTACCGC 1003
1004 GTCAGTGACGTGACCAAAGCCGGACACAGCCTGGAGCTGATTGAGCCCC 1052
1053 TCATCAAGTTCCAGGTGGGACTGAAGAAGCTGAACTTGCATGAGGAGGA 1101
1112 GCATGTCCTGCTCATGGCCATCTGCATCGTCTCCCCAGATCGTCCTGGG 1150
1151 GTGCAGGACGCCGCGCTGATTGAGGCCATCCAGGACCGCCTGTCCAACA 1199
1200 CACTGCAGACGTACATCCGCTGCCGCCACCCGCCCCCGGGCAGCCACCT 1248
1249 GCTCTATGCCAAGATGATCCAGAAGCTAGCCGACCTGCGCAGCCTCAAT 1297
1298 GAGGAGCACTCCAAGCAGTACCGCTGCCTCTCCTTCCAGCCTGAGTGCA 1346
1347 GCATGAAGCTAACGCCCCTTGTGCTCGAAGTGTTTGGCAATGAGATCTC 1395
1396 CTGA

278 Mutant- Nucleotide Sequence.

Nucleotide sequence numbering corresponds to nucleotide sequence # J03258 (National Center for Biological Information, May 2002). Codon change is in **bold.**

125 ATGGCGGCCAGCACTTCCCTGCCTGACCCTGGAGACTTTGACCGGA 170
171 ACGTGCCCCGGATCTGTGGGGTGTGTGGAGACCGAGCCACTGGCTTTCA 219
220 CTTCAATGCTATGACCTGTGAAGGCTGCAAAGGCTTCTTCAGGCGAAGC 268
269 ATGAAGCGGAAGGCACTATTCACCTGCCCCTTCAACGGGGACTGCCGCA 317
318 TCACCAAGGACAACCGACGCCACTGCCAGGCCTGCCGGCTCAAACGCTG 366
367 TGTGGACATCGGCATGATGAAGGAGTTCATTCTGACAGATGAGGAAGTG 415
416 CAGAGGAAGCGGGAGATGATCCTGAAGCGGAAGGAGGAGGAGGCCTTGA 464
465 AGGACAGTCTGCGGCCCAAGCTGTCTGAGGAGCAGCAGCGCATCATTGC 513
514 CATACTGCTGGACGCCCACCATAAGACCTACGACCCCACCTACTCCGAC 562
563 TTCTGCCAGTTCCGGCCTCCAGTTCGTGTGAATGATGGTGGAGGGAGCC 611
612 ATCCTTCCAGGCCCAACTCCAGACACACTCCCAGCTTCTCTGGGGACTC 660
661 CTCCTCCTCCTGCTCAGATCACTGTATCACCTCTTCAGACATTGATGGA 709
710 CTCGTCCAGCTTCTCCAATCTGGATCTGAGTGAAGAAGATTCAGATGAC 758
759 CCTTCTGTGACCCTAGAGCTGTCCCAGCTCTCCATGCTGCCCCACCTGG 807
808 CTGACCTGGTCAGTTACAGCATCCAAAAGGTCATTGGCTTTGCTAAGAT 856
857 ATACCAGGATTCAGAGACCTCACCTCTGAGGACCAGATCGTACTGCTGA 905
906 AGTCAAGTGCCATTGAGGTCATCATGTTGCGCTCCAATGA**GGC**CTTCAC 954
955 CATGGACGACATGTCCTGGACCTGTGGCAACCAAGACTACAAGTACCGC 1003
1004 GTCAGTGACGTGACCAAAGCCGGACACAGCCTGGAGCTGATTGAGCCCC 1052
1053 TCATCAAGTTCCAGGTGGGACTGAAGAAGCTGAACTTGCATGAGGAGGA 1101
1112 GCATGTCCTGCTCATGGCCATCTGCATCGTCTCCCCAGATCGTCCTGGG 1150
1151 GTGCAGGACGCCGCGCTGATTGAGGCCATCCAGGACCGCCTGTCCAACA 1199
1200 CACTGCAGACGTACATCCGCTGCCGCCACCCGCCCCCGGGCAGCCACCT 1248
1249 GCTCTATGCCAAGATGATCCAGAAGCTAGCCGACCTGCGCAGCCTCAAT 1297
1298 GAGGAGCACTCCAAGCAGTACCGCTGCCTCTCCTTCCAGCCTGAGTGCA 1346
1347 GCATGAAGCTAACGCCCCTTGTGCTCGAAGTGTTTGGCAATGAGATCTC 1395
1396 CTGA

143/278 Mutant- Nucleotide Sequence.

Nucleotide sequence numbering corresponds to nucleotide sequence # J03258 (National Center for Biological Information, May 2002). Codon changes are in bold.

125 ATGGCGGCCAGCACTTCCCTGCCTGACCCTGGAGACTTTGACCGGA 170
171 ACGTGCCCCGGATCTGTGGGGTGTGTGGAGACCGAGCCACTGGCTTTCA 219
220 CTTCAATGCTATGACCTGTGAAGGCTGCAAAGGCTTCTTCAGGCGAAGC 268
269 ATGAAGCGGAAGGCACTATTCACCTGCCCCTTCAACGGGGACTGCCGCA 317
318 TCACCAAGGACAACCGACGCCACTGCCAGGCCTGCCGGCTCAAACGCTG 366
367 TGTGGACATCGGCATGATGAAGGAGTTCATTCTGACAGATGAGGAAGTG 415
416 CAGAGGAAGCGGGAGATGATCCTGAAGCGGAAGGAGGAGGAGGCCTTGA 464
465 AGGACAGTCTGCGGCCCAAGCTGTCTGAGGAGCAGCAGCGCATCATTGC 513
514 CATACTGCTGGACGCCCACCATAAGACC**TTC**GACCCCACCTACTCCGAC 562
563 TTCTGCCAGTTCCGGCCTCCAGTTCGTGTGAATGATGGTGGAGGGAGCC 611
612 ATCCTTCCAGGCCCAACTCCAGACACACTCCCAGCTTCTCTGGGGACTC 660
661 CTCCTCCTCCTGCTCAGATCACTGTATCACCTCTTCAGACATTGATGGA 709
710 CTCGTCCAGCTTCTCCAATCTGGATCTGAGTGAAGAAGATTCAGATGAC 758
759 CCTTCTGTGACCCTAGAGCTGTCCCAGCTCTCCATGCTGCCCCACCTGG 807
808 CTGACCTGGTCAGTTACAGCATCCAAAAGGTCATTGGCTTTGCTAAGAT 856
857 ATACCAGGATTCAGAGACCTCACCTCTGAGGACCAGATCGTACTGCTGA 905
906 AGTCAAGTGCCATTGAGGTCATCATGTTGCGCTCCAATGA**GTC**CTTCAC 954
955 CATGGACGACATGTCCTGGACCTGTGGCAACCAAGACTACAAGTACCGC 1003
1004 GTCAGTGACGTGACCAAAGCCGGACACAGCCTGGAGCTGATTGAGCCCC 1052
1053 TCATCAAGTTCCAGGTGGGACTGAAGAAGCTGAACTTGCATGAGGAGGA 1101
1112 GCATGTCCTGCTCATGGCCATCTGCATCGTCTCCCCAGATCGTCCTGGG 1150
1151 GTGCAGGACGCCGCGCTGATTGAGGCCATCCAGGACCGCCTGTCCAACA 1199
1200 CACTGCAGACGTACATCCGCTGCCGCCACCCGCCCCCGGGCAGCCACCT 1248
1249 GCTCTATGCCAAGATGATCCAGAAGCTAGCCGACCTGCGCAGCCTCAAT 1297
1298 GAGGAGCACTCCAAGCAGTACCGCTGCCTCTCCTTCCAGCCTGAGTGCA 1346
1347 GCATGAAGCTAACGCCCCTTGTGCTCGAAGTGTTTGGCAATGAGATCTC 1395
1396 CTGA

Appendix D- Raw Data of Binding Assays- DPM

143-Dec. 18, 2001

Conc-nM	Hot-1	Hot-2	Hot-3	AvgHot	SDhot	XScold-1	XScold-2	XScoldavg	SDXScold	SpBinding
0.125	187.11	163.42	179.01	176.51	12.04	168.89	175.97	172.43	5.01	4.08
0.25	184.28	208.58	188.33	193.73	13.02	52.65	40.50	46.58	8.59	147.15
0.625	520.43	419.18	455.63	465.08	51.28	78.98	113.40	96.19	24.34	368.89
1.25	672.30	573.08	714.83	653.40	72.74	137.70	125.55	131.63	8.59	521.78
2.5	729.00	785.70	751.28	755.33	28.57	216.68	301.73	259.20	60.14	496.13
5	1042.88	1036.80	1048.95	1042.88	6.08	557.00	664.20	615.60	68.73	427.28

143-Jan. 18, 2002

Conc-nM	Hot-1	Hot-2	Hot-3	AvgHot	SDhot	XScold-1	XScold-2	XScoldavg	SDXScold	SpBinding
0.123	58.29	100.26	79.14	79.23	20.99	41.15	35.05	38.10	4.31	41.13
0.246	128.03	111.6	99.91	113.18	14.13	55.30	43.58	49.44	8.29	63.74
0.49	223.3	218.05	175.16	205.50	26.41	59.07	47.6	53.34	8.11	152.17
1.23	1199.93	450	401	683.64	447.79	135.50	237.23	186.37	71.93	497.28
2.46	*1880.47	626.61	580.85	603.73	32.35	294.82	239.74	267.28	38.95	336.45
4.91	748.88	1031.63	705	828.50	177.28	509.13	351.58	435.35	104.33	393.15

*reject by q-test

143-Jan. 29, 2002

Conc-nM	Hot-1	Hot-2	Hot-3	AvgHot	SDhot	XScold-1	XScold-2	XScoldavg	SDXScold	SpBinding
0	0	0	0	0	0.00	0.00	0	0.00	0.00	
0.125	346.91	211.07	240.35	266.11	71.49	59.26	45.11	52.19	10.01	213.93
0.25	552.92	540.78	529.3	544.33	17.09	44.70	52.07	48.39	5.21	495.95
0.625	859.22	993.75	850.39	901.12	80.34	53.10	60.94	57.02	5.54	844.10
1.25	1466.44	1530.26	1593.19	1536.63	53.65	131.12	133.03	132.08	1.35	1404.55
2.5	1664.59	2094.4	2107.58	1955.52	252.04	247.52	211.51	229.52	25.46	1726.01
5	2117.59	2195.57	2082.23	2131.80	57.99	348.58	402.03	375.31	37.79	1755.49

143-Feb. 4, 2002

Conc-nM	Hot-1	Hot-2	Hot-3	AvgHot	SDhot	XScold-1	XScold-2	XScoldavg	SDXScold	SpBinding
0	0	0	0	0.00	0.00	0.00	0.00	0.00	0.00	0.00
0.123	170.86	146.9	175.56	164.11	15.94	39.29	37.51	38.40	1.26	125.71
0.246	178.72	160.12	249.17	195.00	46.97	44.25	63.33	53.79	13.49	142.21
0.49	308.49	295.7	363.7	329.30	47.55	78.85	85.81	82.33	4.92	246.97
1.23	504.59	561.46	485.42	517.49	39.15	157.60	161.38	159.49	2.67	358.00
2.46	950.38	872.19	953.19	925.25	45.98	414.53	540.04	477.29	88.75	447.97
4.91	1015.62	1030.04	974.78	1016.81	42.64	424.11	381.39	402.75	30.21	614.06

278-Jan 8, 2002

Conc-nM	Hot-1	Hot-2	Hot-3	AvgHot	SDhot	XScold 1	XScold-2	XScoldavg	SDXScold	SpBinding
0	0	0	0	0.00	0.00	0.00	0.00	0.00	0.00	0
0.125	834.3	695.6	933.525	821.48	118.98	164.03	125.55	144.79	27.21	676.6875
0.25	1585.575	1686.825	1808.325	1693.58	111.53	176.18	251.10	213.64	52.98	1479.938
0.625	4201.875	3952.8	3491.1	3881.93	360.65	763.43	716.85	740.14	32.93	3141.788
1.25	5761.375	5748.975	6245.1	5925.15	277.56	1711.13	1490.40	1600.76	155.08	4324.388
2.5	9659.25	9724.05	10080.45	9821.25	226.80	1852.88	2379.38	2116.13	372.29	7705.125
5	9037.575	13051.13	16525.25	12904.65	3795.96	5295.38	3578.18	4436.78	1214.24	8467.875

278-Feb 4, 2002

ConcnM	Hst-1	Hst-2	Hst-3	AvgHst	SDhst	XScold-1	XScold-2	XScoldavg	SDXScold	SpBinding
0	0	0	0	0.00	0.00	0.00	0.00	0.00	0.00	0
0.123	141.38	125.17	126.59	131.05	8.98	52.24	63.73	57.99	8.12	73.06167
0.245	112.03	176.16	187.12	158.44	40.55	74.20	86.55	80.38	8.74	78.05866
0.49	252.71	264.17	508.48	345.12	141.48	98.70	125.01	111.86	18.60	233.265
1.23	501.7	572.94	529.11	534.58	35.98	150.76	233.44	192.10	58.46	342.4833
2.46	903.79	1006.78	926.74	947.44	52.17	298.13	360.70	329.92	47.78	620.5217
4.91	1253.59	1206.27	1375.55	1278.47	87.35	661.91	575.82	618.87	53.80	664.6083

278-March 5, 2002

ConcnM	Hst-1	Hst-2	Hst-3	AvgHst	SDhst	XScold-1	XScold-2	XScoldavg	SDXScold	SpBinding
0	0	0	0	0	0.00	0.00	0	0.00	0.00	0.00
0.1375	262.2	332.11	167.42	253.91	82.66	58.51	67.87	63.19	6.62	190.72
0.275	331.25	349.99	383.71	354.98	26.58	87.33	104.73	96.03	12.30	258.95
0.55	729.53	616.5	707.68	685.24	58.82	94.61	173.10	133.86	55.50	551.38
1.29	902.05	1285.28	1042.12	1076.48	193.91	229.02	285.02	257.02	39.60	819.46
2.58	1090.43	1280.09	1317.76	1229.43	121.84	366.20	425.32	395.76	41.80	833.67
4.98	1414.74	2912.21	1863.65	2063.54	768.48	830.11	1625.85	1227.99	552.68	835.55

278-March 13, 2002

ConcnM	Hst-1	Hst-2	Hst-3	AvgHst	SDhst	XScold-1	XScold-2	XScoldavg	SDXScold	SpBinding
0	0	0	0	0.00	0.00	0.00	0.00	0.00	0.00	0.00
0.1375	85.11	107.33	83.84	92.09	13.21	38.37	55.17	47.27	12.59	44.82
0.275	169.23	133.17	160.9	154.43	18.88	77.08	53.55	65.32	16.63	89.11
0.55	264.34	239.55	286.24	263.38	23.35	125.14	235.04	180.09	77.71	83.29
1.29	418.35	501.14	319.74	413.08	90.82	202.19	264.36	233.28	43.95	179.81
2.58	853.09	549.88	1250.3	884.42	351.26	300.15	433.07	366.61	93.99	517.81
4.98	776.75	1073.66	344.9	731.77	366.46	821.73	816.14	818.94	2.54	-88.17

143278-Jan. 18

ConcnM	Hst-1	Hst-2	Hst-3	AvgHst	SDhst	XScold-1	XScold-2	XScoldavg	SDXScold	SpBinding
0	0	0	0	0.00	0.00	0.00	0.00	0.00	0.00	0.00
0.123	102.67	54.5	72.13	76.43	24.37	40.44	37.86	39.15	1.82	37.28
0.245	93.62	97.47	89.99	93.69	3.74	69.01	55.96	62.99	8.52	30.71
0.49	191.32	138.25	129.47	153.01	33.46	80.85	45.17	63.01	25.23	90.00
1.23	253.55	291.39	291.4	282.11	16.03	104.36	122.60	113.48	12.90	168.63
2.46	463.1	533.57	352.28	449.65	91.39	232.27	165.25	198.76	47.39	250.89
4.91	651.84	633.79	680.21	655.61	23.81	375.88	327.21	351.55	34.41	307.07

143278-Jan. 29

ConcnM	Hst-1	Hst-2	Hst-3	AvgHst	SDhst	XScold-1	XScold-2	XScoldavg	SDXScold	SpBinding
0	0	0	0	0.00	0.00	0.00	0.00	0.00	0.00	0.00
0.123	70.91	20.14	174.53	88.53	78.69	32.21	36.33	34.27	2.91	54.26
0.245	240.76	248.2	238.22	242.39	5.19	40.12	30.89	35.51	6.53	206.89
0.49	355.93	359.53	390.32	368.60	18.89	58.04	50.24	54.14	5.52	314.46
1.23	600.63	661.97	654.51	639.04	33.47	87.79	139.48	113.64	36.55	525.40
2.46	843.51	843.31	786.92	824.58	32.61	176.55	160.27	178.42	2.62	646.17
4.91	1162.88	1462.82	1014.81	1210.17	222.80	283.42	355.60	319.51	51.04	890.66

143278-March 4, 2002

Conc-nM	Hot-1	Hot-2	Hot-3	Avg Hot	SD hot	XScold-1	XScold-2	XScold avg	SD XScold	Sp Binding
0	0	0	0	0.00	0.00	0.00	0.00	0.00	0.00	0.00
0.1375	28.97	*919.7	155.17	92.07	89.24	97.10	107.27	102.19	7.19	-10.12
0.275	528.39	552.53	532.73	537.88	12.67	233.84	169.52	201.68	45.48	336.20
0.55	1293.84	1513.62	1514.47	1440.64	127.14	455.61	421.94	438.78	23.81	1001.87
1.29	2214.76	2231.83	2147.65	2198.08	44.50	1412.62	858.22	1135.42	392.02	1062.66
2.58	3061	4268	3428	3585.67	618.75	2536.61	1879.72	2208.17	464.49	1377.50
4.98	4652	4425	4686	4587.67	141.90	2837.50	3533.77	3185.64	492.34	1402.03

*reject by Q test

143278-March 18, 2002

Conc-nM	Hot-1	Hot-2	Hot-3	Avg Hot	SD hot	XScold-1	XScold-2	XScold avg	SD XScold	Sp Binding
0	0	0	0	0.00	0.00	0.00	0.00	0.00	0.00	0.00
0.1375	66.5	124.5	118.5	103.17	31.90	30.50	77.50	54.00	33.23	49.17
0.275	108.5	132.5	102.5	113.83	16.29	61.00	52.00	56.50	6.36	57.33
0.55	279.5	226.5	208.5	237.50	37.72	82.50	91.50	87.00	6.36	150.50
1.29	343	281	453	359.00	87.11	205.50	140.50	173.00	45.96	186.00
2.58	358.5	499	545.5	467.67	97.36	377.50	343.50	360.50	24.04	107.17
4.98	873.5	1999	1522.5	1465.00	564.95	529.50	605.50	567.50	53.74	897.50

WT- Nov. 27, 2001

Conc-nM	Hot-1	Hot-2	Hot-3	Avg Hot	SD hot	XScold-1	XScold-2	XScold avg	SD XScold	Sp Binding
0	0	0	0	0.00	0.00	0.00	0	0.00	0.00	0.00
0.125	87.075	103.275	101.25	97.20	8.83	60.75	28.35	44.55	22.91	52.65
0.25	133.65	157.95	135.675	142.43	13.48	48.60	58.725	53.66	7.16	88.76
0.625	427.275	321.975	451.575	400.28	68.89	143.78	125.55	134.66	12.89	265.61
1.25	469.8	504.225	554.85	509.63	42.78	348.30	174.15	261.23	123.14	248.40
2.5	716.85	639.9	694.575	683.78	39.60	277.43	253.125	265.28	17.18	418.50
5	1050.975	1071.225	1111.725	1077.98	30.93	613.58	686.475	650.03	51.55	427.95

WT March 4

Conc-nM	Hot-1	Hot-2	Hot-3	Avg Hot	SD hot	XScold-1	XScold-2	XScold avg	SD XScold	Sp Binding
0	0	0	0	0.00	0.00	0.00	0	0.00	0.00	0.00
0.1375	99.27	84.13	71.55	84.98	13.88	31.81	39.08	35.45	5.14	49.54
0.275	319.95	632.02	216.72	389.56	216.22	188.06	210.92	199.49	16.16	190.07
0.55	680.47	505.82	928.6	708.30	211.95	149.12	476.83	312.98	231.73	395.32
1.29	781.47	749.15	910.86	813.83	85.57	270.06	197.5	233.78	51.31	580.05
2.58	1143.42	1054.54	1345.32	1181.09	149.01	938.45	457.56	698.01	340.04	483.09
4.98	1599.9	1390.92	1520.73	1500.52	101.02	781.64	725	753.32	40.05	747.20

WT March 5

Conc-nM	Hot-1	Hot-2	Hot-3	Avg Hot	SD hot	XScold-1	XScold-2	XScold avg	SD XScold	Sp Binding
0	0	0	0	0.00	0.00	0.00	0.00	0.00	0.00	0.00
0.1375	279.02	241.39	249.28	256.56	19.84	63.05	57.68	60.37	3.80	196.20
0.275	399.99	460.21	430.04	428.75	25.27	82.78	147.10	114.94	45.48	311.81
0.55	1184.04	585.34	725.13	831.50	313.20	313.90	133.04	223.47	127.89	608.03
1.29	1818.79	1507.84	741.03	1355.89	554.72	409.74	446.56	429.15	27.45	926.74
2.58	1435.54	1533.56	1435.31	1468.14	55.66	450.01	743.19	596.60	207.31	871.54
4.98	1735.37	2149.42	2293.87	2059.55	289.89	898.29	792.24	845.27	74.99	1214.29